INTERNATIONAL JOURNAL OF ENERGY RESEARCH
Int. J. Energy Res. 2011; **35**:929–963
Published online 6 April 2011 in Wiley Online Library (wileyonlinelibrary.com). DOI: 10.1002/er.1833

REVIEW

A review on devolatilization of coal in fluidized bed

Ramesh C. Borah[1,2,*,†], Pallab Ghosh[2] and Paruchuri G. Rao[1]

[1]Chemical Engineering Department, Northeast Institute of Science and Technology, Jorhat-785006, Assam, India
[2]Chemical Engineering Department, Indian Institute of Technology Guwahati, Guwahati-781039, Assam, India

SUMMARY

Devolatilization is an important step in fluidized bed combustion and gasification of coal. 'Devolatilization' is a general term that signifies the removal of volatile matters from the coal matrix. It is an extremely important step because the combustion of volatile matter can account for 50% of the specific energy of fluidized bed combustion of a high-volatile coal. Significant insights into the complex physicochemical phenomena that occur during devolatilization have been obtained in the recent years. This review focuses on the devolatilization of coal in an inert gas, air, and oxygen-enriched air, with emphasis on the effects of the operating parameters (e.g. temperature, heating rate, pressure, and gas velocity) on the yield of volatile matter. Particle size, oxygen content of the fluidizing gas, volatile content of coal and specific heat are some of the other important parameters for the devolatilization of coal. This review also explains the development and application of structural and empirical models. The structural models (e.g. FG-DVC and CPD models) are fairly complex. However, they can accurately predict the yields of gas and tar. It is observed from the review of the literature that the mechanism of coal devolatilization needs further study. Although the shrinking-core model can describe the devolatilization in the beginning and toward the end of the process, major deviations are often observed. The economic studies reveal that the capital cost of fluidized bed combustion reduces upon doubling the capacity. Some problems associated with bubbling fluidized bed combustion (e.g. the increase in freeboard temperature) have been explained with the present knowledge of devolatilization. Copyright © 2011 John Wiley & Sons, Ltd.

KEY WORDS

coal; combustion; devolatilization; fluidized bed; gasification

Correspondence

*Ramesh C. Borah, Chemical Engineering Department, Northeast Institute of Science and Technology, Jorhat-785006, Assam, India.
†E-mail: borahrc@rrljorhat.res.in

Received 27 July 2010; Revised 21 November 2010; Accepted 23 January 2011

1. INTRODUCTION

Coal has fueled the industrial revolution in the previous two centuries. The primary energy resource in many countries (e.g. India) is not oil, but coal. To illustrate, coal accounted for 53% of India's energy consumption in 2007, and the demand is set to grow over the ensuing decades. Because coal is cheap and abundant domestically, it may seem like the perfect solution to the energy requirements of these countries. However, coal is the most-polluting fossil fuel. The conventional methods of utilization of coal have low efficiency and high pollution characteristics in comparison with oil and natural gas. A few clean coal technologies, such as Integrated Gasification Combined Cycle (IGCC) and Fluidized Bed Combustion (FBC), have been identified as viable technologies to circumvent these problems. A fundamental understanding of the physical and chemical processes involved in the modern coal conversion technologies is necessary to achieve a higher efficiency and less adverse impact on the environment.

This article presents a review of the literature on the devolatilization of coals pertinent to the fluidized bed gasification and combustion processes. Emphasis is given on the parameters that are important to improve the efficiency of fluidized bed coal combustion and gasification. Special attention is given to the coals that contain high amounts of volatile matter so that this article can be helpful for the design and control of commercial fluidized bed combustors or pyrolyzers that use this type of coals. In this review, the mechanism of devolatilization, the nature of transformation that occurs inside the coal particles, and the products of devolatilization are discussed. The devolatilization models available in the literature are reviewed focusing on the type of the model, chemical kinetics of coal devolatilization, and the devolatilization of large particles. This article explains the present state of knowledge on coal devolatilization, develops

a perspective of the technology used, and explains the scope of future work.

2. FUNDAMENTAL ASPECTS OF COAL DEVOLATILIZATION

2.1. Chemical structure of low-rank coals

It is necessary to understand the chemical structure of the low-rank coals to explain the structural changes which occur during coal devolatilization. The chemical structure of coal depends upon the process through which it has formed. Coal originates from peat, which is formed from plant matter that deposits or grows in swamps. The transformation from peat to coal occurs via the application of heat and pressure. Generally, the peat deposit is buried under sediments (e.g. sands and clays), and the thickness of this overburden determines the temperature and pressure to which the deposit is exposed. This transformation process is thermodynamically favorable, and it is called *coalification*.

Peat is composed of a significant amount of lignin and cellulose, which is present in the original plant deposits. In the first stage of coalification, dewatering and decomposition of the hydrophilic functional groups of peat occurs because of the increase in pressure and temperature. The cellulose begins to undergo decomposition while the lignins are preserved, and they become concentrated in peat. Formation of the humic acid functional group follows to which cations, such as Na^{+}, Ca^{+2}, Mg^{+2}, Fe^{+3} and Al^{+3}, can bind to form humate. The ensuing gelation stage involves the formation of colloidal humic gels, which precipitate in void spaces resulting in the reduction of the porosity of peat. As coalification progresses, the oxygen content of the coal is gradually reduced via decomposition of the carboxyl ($-COOH$), methoxyl ($-OCH_3$), and carbonyl ($>C=O$) functional groups, as well as ring oxygen. The final stages of coalification involve the condensation of humic acids to larger molecules and the removal of aliphatic and alicyclic functional groups. This chemical change indicates that the coal gradually becomes more and more aromatic and carbon-rich in nature [1].

A number of hypothetical models of the structure of coals have been developed. A typical structure proposed for bituminous coal is depicted in Figure 1. It is observed in this figure that the coal is composed of groups of aromatic ring clusters that are cross-linked

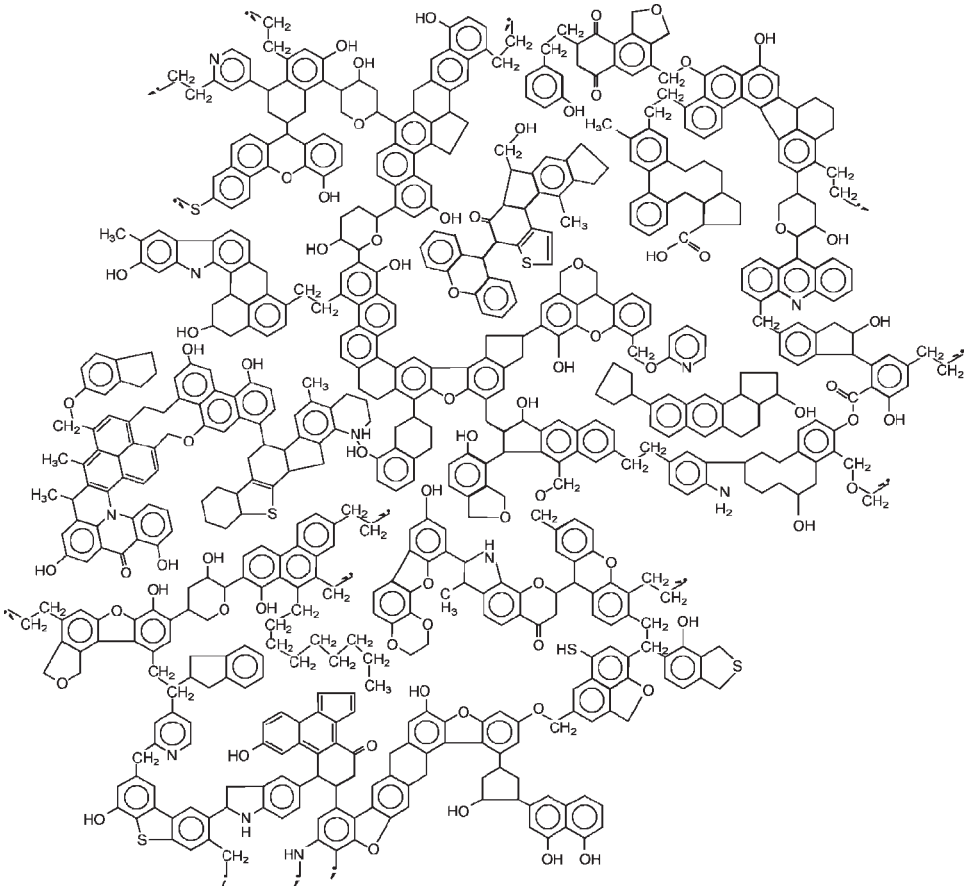

Figure 1. Structure of bituminous coal [2].

by aliphatic or ether bridges. The size of the aromatic ring varies from one to multiple rings per cluster, and a variety of functional groups (e.g. carbonyl, carboxyl, ether, and phenol groups) are attached to the rings. The aromatic rings may be mono-substituted with heteroatoms, such as nitrogen, sulfur, or carbon. This covalently bonded chain of aromatic ring clusters is known as the *immobile phase*. Small interstices or holes are present throughout this continuous chain of aromatic ring clusters, in which smaller molecules may be trapped. These molecules are generally aliphatic in nature. However, minerals such as quartz (SiO_2) and kaolinitic clays (e.g. $Al_2Si_2O_4(OH)_4$) may also be present. These molecules constitute the so-called *mobile phase*. Inorganic materials, such as Na, K, Ca, Al, and Fe, are also found within the coal structure. They are typically attached to carboxyl (or similar) groups, or included as chelate complexes [3–5].

2.2. General mechanism of coal devolatilization

The physicochemical transformations, which occur during devolatilization, have been investigated by a number of workers [3–7]. They have proposed various mechanisms to describe the transformations. The mechanism proposed by van Heek and Hodek [5] for the devolatilization of coal is shown schematically in Figure 2. According to this mechanism, the coal degradation process starts with the desorption of moisture and some light gases (mainly methane and nitrogen) at $\sim$393 K. On further heating, distillation of the mobile phase occurs at temperatures above 523 K leading to the formation of tar, particularly the aliphatic tar components. At temperatures greater than 673 K, degradation of the immobile phase starts resulting in the formation of the aromatic tar fractions, a number of light gases (e.g. H_2O, CO, and CO_2), and low-molecular-weight hydrocarbons (e.g. CH_4, C_2H_4, C_2H_6, C_3H_6, and C_3H_8). Finally, condensation of the vaporized aromatics to char occurs at temperatures above 873 K. This is associated with the decomposition

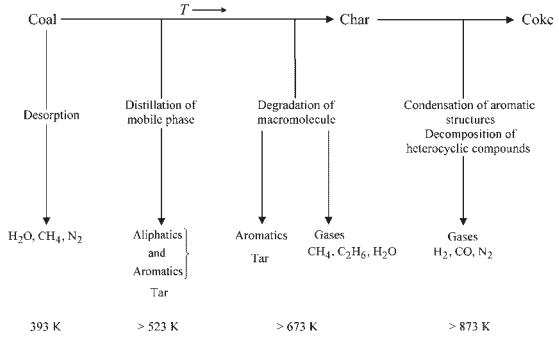

Figure 2. Main reactions that occur during coal pyrolysis as per the mechanism of devolatilization proposed by van Heek and Hodek [5].

of heterocyclic compounds yielding N_2, H_2S, and CO. Hydrocracking of the aromatics also occurs, which releases H_2 [5].

Solomon *et al.* [4] proposed the following mechanism which describes the formation of the tar and char fractions.

Stage 1: Depolymerization occurs by the rupture of weaker bridges in the coal macromolecule to release smaller fragments, which make up the metaplast.

Stage 2: Repolymerization (i.e. cross-linking) of the metaplast molecules takes place.

Stage 3: Transport of lighter molecules away from the surface of the coal particles occurs by combined vaporization, convection, and gas phase diffusion.

Stage 4: Internal transport of the molecules to the surface of the coal particles takes place by convection, by diffusion into the pores of non-softening coals, and by liquid phase diffusion or bubble transport in softening coals. Char is formed from the unreleased or recondensed fragments. Various amounts of loosely bound guest molecules, usually associated with the extractable material, are also released during devolatilization.

This mechanism is similar to that proposed by van Heek and Hodek [5] except that the metaplast stage described here is called *mobile phase* by van Heek and Hodek [5]. Solomon *et al.* [3] proposed a structural model for sub-bituminous coal, which is shown in Figure 3. Comparing Figure 3(a) and (b), it can be observed that the aliphatic bonds denoted by (2) in Figure 3(a) have ruptured, and the carbon radicals formed in the process picked up the hydrogen radicals to form either methyl or ethyl groups. The hydrogen radicals have been generated by the dehydrogenation of a hydroaromatic ring such as that shown in the lower right side of the molecule in Figure 3(a). These two breakages of aliphatic bonds result in the fragments which are light enough to evolve as tars [3].

The aliphatic ether bond denoted by (1) in Figure 3(a) has been disrupted leading to the formation of a hydroxyl group via a hydrogen radical, which is depicted in Figure 3(b). At the position labeled (3) in Figure 3(b), condensation of two hydroxyl groups has resulted in the formation of a second aromatic ether bond and the release of H_2O. Other independent transformations have occurred such as the decomposition of the carboxyl group depicted at the center of Figure 3(a) to yield CO_2, an aliphatic ether bond has been ruptured releasing a methyl group as CH_4 (on the left side of Figure 3(a)), and a mercaptan in the lower right corner of Figure 3(a) has detached to form H_2S [3]. These transformations are similar to those described in the mechanism proposed by van Heek and Hodek [5].

The structural changes shown in Figure 3 are those that occur during primary devolatilization. During this stage, decomposition of the macromolecular structure of the coal takes place. The disintegrated fragments produced from primary devolatilization are small, which can

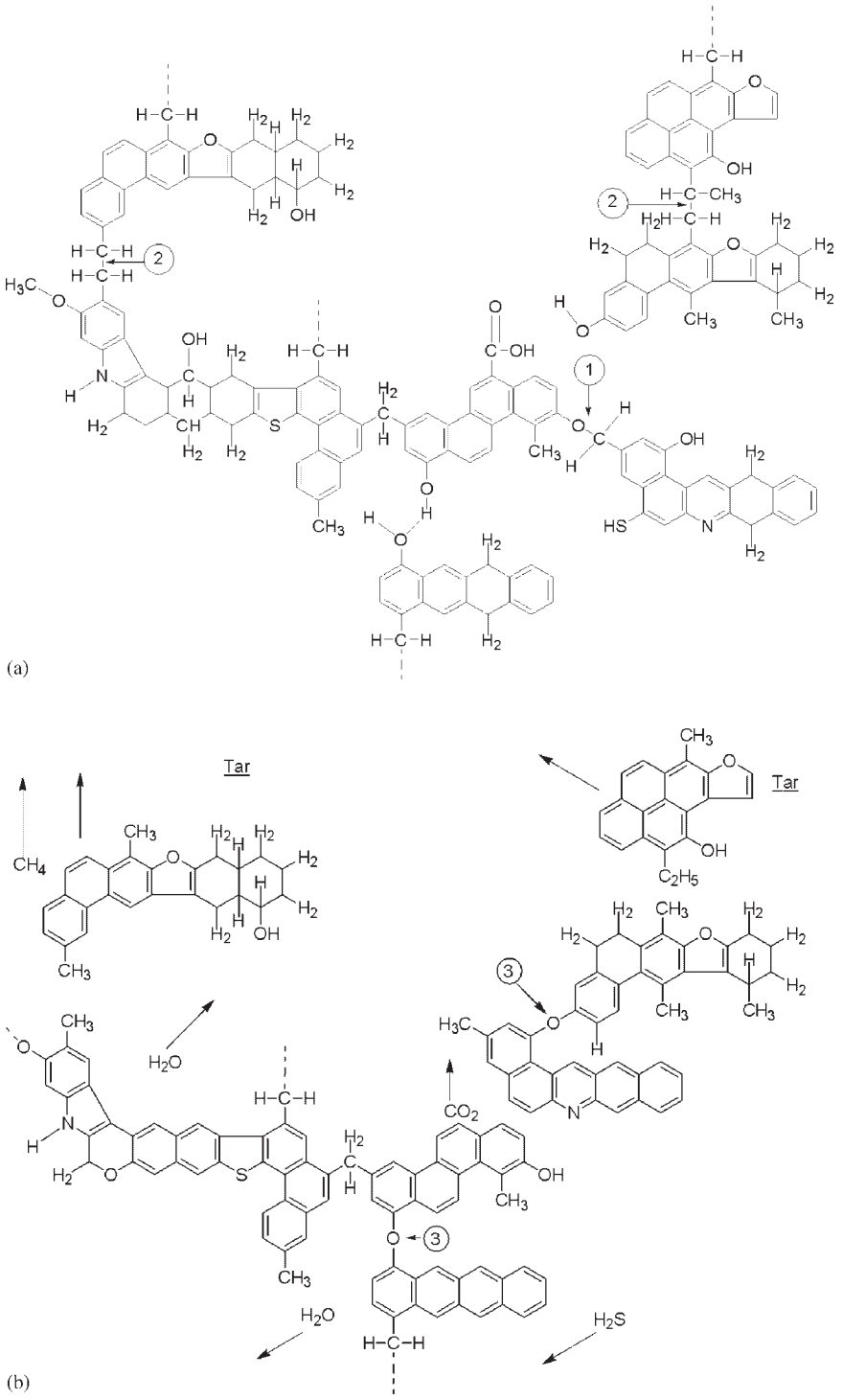

Figure 3. Hypothetical chemical structure of a sub-bituminous coal and the change in structure during devolatilization [3].

escape from the coal surface [8]. *Secondary devolatilization* is the decomposition of the components evolved during primary devolatilization in the vapor phase.

Pather and Al-Masry [9] have proposed a mechanism of coal devolatilization that involves three stages as described below.

Stage 1: Release of primary volatile matters at the solid–gas interface occurs due to thermal decomposition.

Stage 2: Secondary volatile matters are produced during the diffusion of gaseous products through the pores within the coal particles.

Stage 3: Tertiary volatile matters are produced due to the decomposition reactions occurring in the void spaces between the particles.

The secondary decomposition described in Stages 2 and 3 by Pather and Al-Masry [9] is essentially the transformation of tar species, which are formed during primary devolatilization through the reactions such as tar cracking, dehydrogenation, aromatization, and condensation. The lighter fraction of primary volatile matter is generally stable. However, at the higher temperatures, decomposition of benzylic compounds has been reported in the literature [10].

Several works have studied the secondary decomposition of tar [10–14]. These works have focused on the rationalization of the influence of various operating parameters. A mechanism of tar decomposition was proposed by Hesp and Waters [10] based on a bench-scale study of decomposition of tar produced in a carbonizer when passed through a bed of coke in the temperature range of 973–1273 K. This mechanism suggests that tar decomposition takes place in three distinct phases, which are summarized below.

Phase 1: This phase involves rapid decomposition into gas and carbon. The amount of tar decomposing to gas is directly proportional to the temperature of cracking, and the time required is inversely proportional to temperature. Gas is the main product, which indicates that the gas-forming reactions are quicker than the reactions that form carbon.

Phase 2: This phase involves the formation of carbon by the secondary decomposition of gas. Hydrogen is also formed, accompanied by the slow decomposition of the tar, which escapes the cracking reactions in the first phase. Since a major part of the total carbon is obtained in this phase, it is called *the phase of carbon formation*. It is much longer than the first phase, and its duration is inversely proportional to the temperature of cracking.

Phase 3: The third phase involves slow evolution of gas from tar after the first two phases of decomposition. The amount of gas formed in the third phase is directly proportional to the amount of tar entering into the third phase, and is inversely proportional to the temperature of cracking.

Therefore, it is evident that the devolatilization process is related to the structure of the parent coal. The structural and mechanistic models form the basis on which the observations regarding the influence of various operating parameters on the devolatilization can be analyzed. Experiments can be designed to ascertain the controlling mechanism for fluidized bed combustion and gasification processes.

2.3. Effects of various parameters on coal devolatilization

As the coal devolatilization process is complex in nature, several parameters have direct and indirect influence over the nature and composition of the products evolved during devolatilization. Of these parameters, the most significant are the rank of the coal, particle size, heating rate, gaseous environment, temperature, pressure, superficial gas velocity, oxygen concentration, fragmentation of coal, and the presence of cations that have catalytic effect on coal devolatilization. Moisture content of coal is related to its rank. The moisture content decreases as the rank of the coal increases. For low-rank coals, the moisture content is high, and the removal of moisture plays an important role in devolatilization. The majority of works reported so far in the literature is related to the combustion of pulverized coal. However, recently, efforts have been made to study the devolatilization of large coal particles relevant for fluidized bed coal combustion and gasification. The effects of some of these parameters are discussed in detail in the following sections.

2.3.1. Effect of rank of coal. The rank of coal depicts the stage at which the coal has reached on its coalification path. With increase in the rank, the carbon content increases, and the moisture and volatile matter contents decrease. The volatile matter released by lignite contains a large proportion of oxygen compounds, whereas the same released by the bituminous coals contains a large proportion of hydrocarbons. Lignites release a high percentage of volatile matter at temperatures as low as 773 K [15–17]. The yield of devolatilization reaches the proximate volatile content of coal in the temperature range of 973–1173 K. There is no effect of particle size on the yield of volatile matter for lignites. Furthermore, the total yield of volatile matter does not exceed the proximate volatile content. However, in case of bituminous and anthracite coals, the total yield of volatile matter often exceeds the proximate volatile content of coal [17]. Also, the yield of volatile matter increases with increase in particle size for bituminous and anthracite coals [15].

2.3.2. Effect of temperature on devolatilization. Temperature is an important parameter for any coal devolatilization process [18]. The effects of temperature on the yields of tar, gas, and char have been reported by Tyler [19]. It is observed from his work that the yield of C_1–C_3 hydrocarbons increases linearly with the increase in temperature, while the total volatile yield increases significantly up to $\sim$1000 K, and then becomes invariant with temperature. Several other investigators have corroborated this behavior [10–12,14,20–22]. It is evident from

the results shown in Figures 4–7 that the yields of the products have different trends as the temperature of devolatilization increases. Xu and Tomita [12] have reported that the yield of product is relatively constant up to 873 K. This is also observed in the results reported by Hesp and Waters [10], Tyler [21], and Cliff *et al.* [22] for several volatile products. The yield of tar increases with temperature up to 873 K, and subsequently decreases by almost 50% beyond this temperature [10,12,22]. Xiong *et al.* [23] have studied the pyrolysis of lignite and bituminite in a fluidized bed reactor. They have reported that the yield of tar is highest in the temperature range of 823–923 K. They have reported a tar yield of 11.4% (by weight) for bituminite and 6.4% for lignite on the dry ash-free (daf) coal basis. They have used simulated pyrolysis gas as the reaction atmosphere. Considering the mechanisms of primary and secondary decomposition discussed earlier, this trend suggests that at temperatures lower than 873 K, secondary decomposition reactions are minimal and primary decomposition is dominated by Stage 1 reactions. Above 873 K, primary decomposition via Stages 2–4 begins to become more significant, as does the extent of the secondary decomposition reactions.

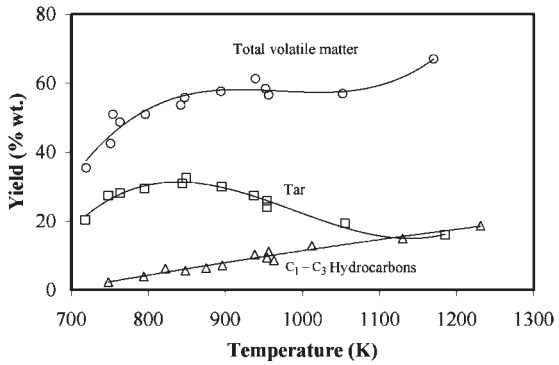

Figure 4. Effect of temperature on the yields of tar, total volatile matter, and C_1–C_3 hydrocarbons [19].

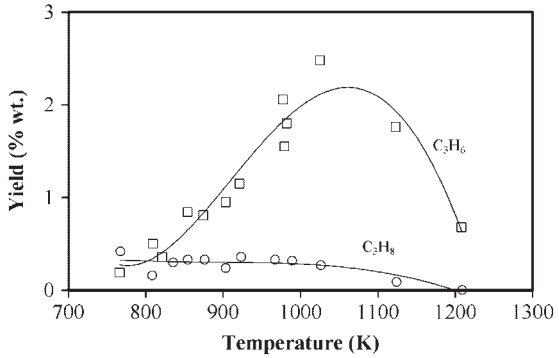

Figure 5. Effect of temperature on the yields of C_3H_6 and C_3H_8 [19].

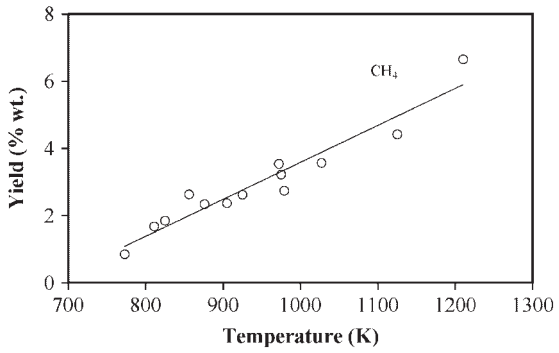

Figure 6. Effect of temperature on the yield of CH_4 [19].

Xu and Tomita [12] monitored the yields of gases produced when the primary volatiles from a bituminous coal were allowed to pass through a packed bed reactor at various operating temperatures. This enabled them to investigate the extent of the secondary reactions. The yields of the products are summarized in Table I for a gas phase residence time of 7 s. Table I confirms that the minimal secondary decomposition reactions occur below 873 K. Immediately above 873 K, there is a noticeable increase in the yields of H_2, CO, CH_4, C_2H_4, C_3H_6, and benzene. It is apparent that the secondary decomposition reactions of Phase 2 occur due to the increase in coke formation. The yields of CO_2 and H_2O remain rather constant, whereas the yields of the majority of the remaining gases tend to decrease steadily with temperature. These results also show that at 1173 K, only H_2, CO, CO_2, H_2O, CH_4, C_2H_4, and benzene are present to a significant level. This agrees with the observations of several other workers [10,21,22]. The decrease in the yield of the heavier products indicates that secondary decomposition has taken place. The products are not limited to hydrogen. They also contain methane and ethylene, and to a lesser extent, benzene. The formation of coke

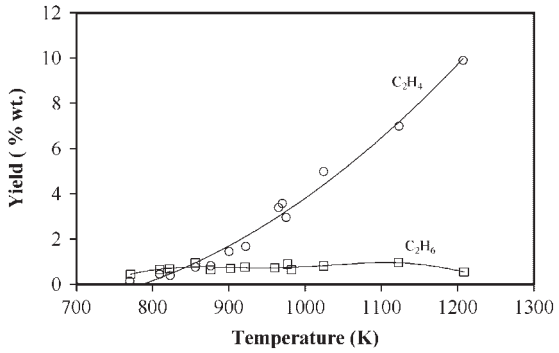

Figure 7. Effect of temperature on the yields of C_2H_4 and C_2H_6 [19].

Int. J. Energy Res. 2011; **35**:929–963 © 2011 John Wiley & Sons, Ltd.
DOI: 10.1002/er

Table I. Effect of temperature on the yield of products from a bituminous coal [12].

	Yield (weight %)									
T (K)	H_2	CO	CO_2	H_2O	CH_4	C_2H_4	C_2H_6	C_3H_6	C_3H_8	C_4
773	0.4	2.1	1.7	4.0	3.5	0.8	0.90	0.60	0.30	0.50
873	0.4	2.0	1.6	4.3	3.6	0.9	1.00	0.80	0.30	0.60
973	0.5	2.5	1.4	4.1	4.6	1.9	1.00	1.30	0.20	0.70
1073	0.6	2.7	1.9	4.1	5.4	3.0	0.50	0.40	0.00	0.20
1173	0.9	3.4	2.0	3.6	5.7	2.0	0.05	0.03	0.00	0.04
	C_5–C_6	Benzene	Toluene	Xylene	Phenol	Cresol	Xylenol	Coke		
773	0.60	0.1	0.3	0.3	0.40	0.6	0.6	1.2		
873	0.70	0.2	0.3	0.3	0.40	0.6	0.6	1.4		
973	0.40	0.3	0.4	0.4	0.40	0.6	0.4	2.3		
1073	0.10	0.8	0.5	0.5	0.30	0.3	0.1	3.1		
1173	0.03	1.3	0.2	0.2	0.04	0.1	0.0	4.9		

indicates that the Phase 3 decomposition has not been reached, because this phase is characterized by the gradual release of H_2 and CO, and only becomes predominant at longer residence times [10].

Calkins *et al*. [24] examined the thermal cracking of a typical coal tar vapor by measuring the yields of the gases after passing the tars produced at 873 K through a tar cracker. The thermal cracking reactions were investigated by varying the cracker temperature. They observed that the temperature at which cracking became apparent decreased with the increase in the length of the carbon chain. Thermal cracking of 1-butene was observed at 923 K, whereas the minimum cracking temperature was $\sim$1273 K for methane. It is interesting to note that the yield of ethylene (which is a major product of the thermal cracking reactions) increased consistently with temperature.

From the foregoing discussion, it can be concluded that the trends observed in the yield and the distribution of the products of devolatilization with variation of temperature can be rationalized using the mechanisms proposed by Solomon *et al*. [3], and Hesp and Waters [10] for the primary and secondary decomposition reactions.

2.3.3. Effect of pressure. The effect of operating pressure on coal devolatilization is most notably characterized by the decrease in the tar yield and decrease in the total yield of the volatile matter [20,25]. Ladner [25] noted that the decrease in the yield of tar was accompanied by an increase in the yield of char. Suuberg *et al*. [20] and Ladner [25] have reported that the total yield of the hydrocarbon gases increased with increase in pressure, which has been supported by Gokhale *et al*. [26]. A significant amount of additional gases is produced at the higher pressures, which can be attributed to the increase in methane formation [25,26]. This suggests that the devolatilization at high pressures is governed by Stages 3 and 4 (primary), and Phase 2 (secondary) decomposition reactions. It should be noted that Phase 2 has been suggested because the increase in the total yield of char indicates that the process is in the phase of char formation. Shin *et al*. [27] have studied the gasification of bituminous coal at high pressure in inert and oxidizing atmospheres. They have observed a decrease in carbon conversion in inert atmosphere with increase in the pressure.

Increase in external pressure during devolatilization results in a decrease in the differential pressure between the pores and the external particle surface. This suggests that the driving force for the transport of the products out of the particle is reduced, resulting in a longer residence time in the pores. This is further enhanced by the decrease in the molecular diffusivity of the product species arising from the increased pressure. Ultimately, the slowdown of the transport processes within the particle extends the contact time of the products with the coal structure, and exposes them to a greater opportunity for the secondary reactions to occur. Also, the thermal cracking reactions of the tar species along with condensation to form char predominate. This leads to the reduction in the yield of tar, and increase in the yields of the hydrocarbon gases and char. The primary species formed from the thermal decomposition of the initial coal structure are not significantly altered by the increase in pressure. However, the effect of pressure is manifested during the subsequent transformations. Shin *et al*. [27] have reported that carbon conversion increases in oxidizing atmosphere as the pressure in the system increases. At higher pressure, more oxygen is available for oxidation of carbon and volatile compounds. This is the likely reason for the increase in carbon conversion.

Cho *et al*. [28] have studied gasification of coal at high pressure. They found that carbon conversion and gas concentrations varied linearly with the oxygen/carbon

ratio at temperatures over 1500 K and 1500 kPa pressure. Under these conditions, the reactions are primarily diffusion controlled. The exit carbon conversion was found to vary with the type of coal.

2.3.4. Effect of heating rate. To study the effect of heating rate, other parameters should be kept constant. Study of devolatilization can be performed in different types of reactor, but factors such as gas phase residence time must be kept constant so that the product yields are directly comparable. The most common techniques that have been adopted by various workers for the study of the effect of heating rate are the wire mesh [20] or micro sample strip reactors [29]. Such reactors typically utilize either wire mesh grid or thin heating elements over which the coal sample is thinly dispersed to enable easy escape of the volatile products. Hence, the secondary decomposition is reduced. In these reactors, heating rates employed were in the range of 100–10 000 K s^{-1}. The amount of sample used in these studies was $\sim$20 mg. Niksa *et al.* [29] deduced that the effect of heating rate was not uniform and it was dependent on the pressure of the system. It was found that the increase in heating rate increased the total volatile yield *in vacuo*, and the magnitude of increase was in the range of 10–20% when the heating rate was increased from 100 to 1000 K s^{-1}. At higher pressures, the effect of heating rate was less apparent. This suggests that at high pressure, diffusion processes become dominant and limit the rates of the subsequent chemical kinetics steps (viz., Stages 3 and 4 of primary decomposition). Suuberg *et al.* [20] deduced that the heating rate has a negligible effect on the yields of the products. Ladner [25] reported that the increase in heating rate resulted in an increase in oil and tar yields, and a decrease in the yield of char. Similar results have been reported by Peters and Bertling [30]. Akash *et al.* [31] studied the devolatilization of a bituminous coal in a fixed bed. They observed increase in the loss of volatile matter with increase in the heating rate.

Loison and Chauvin [32], Jones *et al.* [33], Eddinger *et al.* [34], Rau and Robertson [35], Mentser *et al.* [36], and Anthony *et al.* [37] have reported increase in volatile yield with increase in the rate of heating. The heating rate employed in these experiments were in the range of 600–50 000 K s^{-1}. However, this is not feasible for the particle size used in a commercial fluidized bed combustor. Moreover, a single heating rate cannot represent the heating rate of all particles involved in a fluidized bed combustor or gasifier.

Gavalas [38] has compared the results obtained for fixed bed and fluidized bed devolatilization of coals. He found that the yield of tar increased significantly in the fluidized bed rig in comparison with the fixed bed rig. Heating rates are expected to be higher in a fluidized bed rig, which suggests that such heating rates favor tar evolution and limit the secondary reactions. It is likely that the increased heating rate induces a more rapid release of volatile matter from the particles, and accordingly there is a greater internal build-up of pressure within the pore structure. This pressure build-up expels the products from the particles more rapidly and reduces their residence time within the pore structure. This limits the secondary tar cracking and condensation reactions. Stubington and Sasongko [39] have reported a heating rate of 150 K s^{-1} for 2–20 mm diameter coal particles in industrial fluidized bed combustors. They calculated the average heating rate from the time of entry of the particle to the bed up to the time of 95% devolatilization (i.e. 95% of the ultimate mass-loss).

In an oxidizing atmosphere, there can be a large enhancement of heating rate because of the combustion of volatile matter at the surface of the particle, which increases the surface temperature and the heating rate. An increase in the heating rate induces a more rapid release of volatile matter. A rapid release of volatile matter limits the secondary reactions, thereby increasing the yield of volatiles beyond the proximate volatile content of the coal. It has been reported in the literature [40] that the rapid increase in temperature at the high heating rates decreases the residence time of volatile material. It reduces the influence of cracking and more tarry liquid is produced. However, the yield of the light hydrocarbon gases remains nearly constant. It has also been reported in the literature [40] that the increase in the yield of tar with increase in the heating rate is greater for the low-volatile coals than that for the high-volatile coals.

In a recent work, Borah *et al.* [16] have presented photographs of the cross-sections of coal particles pyrolyzed in inert atmosphere and air (Figure 8). It can be observed from Figure 8 that cracks are developed in the coal particle that was pyrolyzed in air. This may be due to the build-up of pressure inside the coal particle as a result of the enhancement in heating rate in the presence of oxygen. This caused an increase in the volume of volatile matter, which developed the cracks. This pressure caused a rapid expulsion of the products from the particles, and reduced their residence time within the pores. Some of the coals fragmented into smaller pieces during devolatilization. The increase in the surface area further enhanced the heating rate, and the yield of volatile matter exceeded to the extent of 25% above the proximate volatile content of the coal [16].

Ross *et al.* [41] measured the time required for the center of a large particle to reach the temperature of the fluidized bed in nitrogen and air. Figure 9 depicts the variation of the average heating rate with particle diameter in air at 1123 K in a fluidized bed. It is observed from this figure that the average heating rate decreased with the increase in particle diameter. The reason for this decrease is as follows. Coal is not a good conductor of heat, and there exists a temperature gradient from the surface of the particle to its center.

Int. J. Energy Res. 2011; **35**:929–963 © 2011 John Wiley & Sons, Ltd.
DOI: 10.1002/er

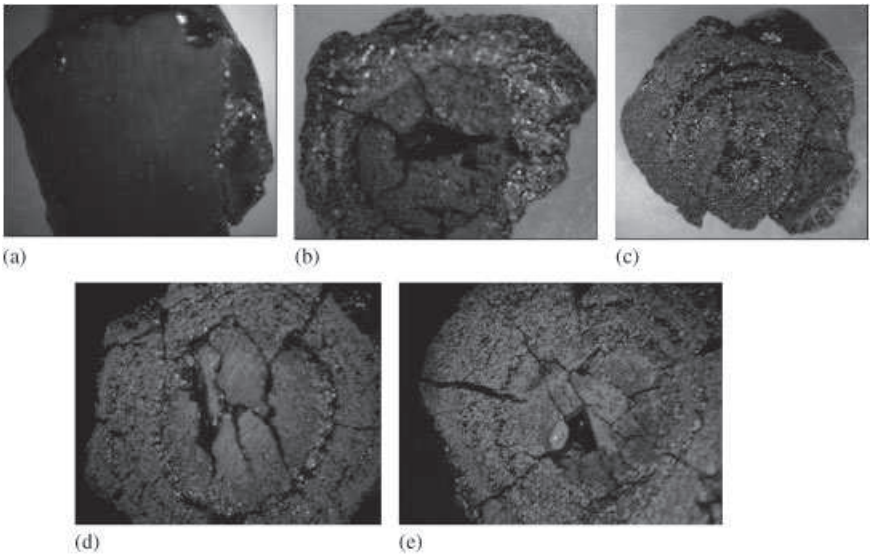

Figure 8. Cross-sectional views of Baragolai A (Assam, India) coal particles at different stages of devolatilization: (a) particle before placing into the basket, (b) after 50 s in argon atmosphere, (c) after 60 s in argon atmosphere, (d) after 40 s in air, and (e) after 60 s in air. Magnification = 15 × [16].

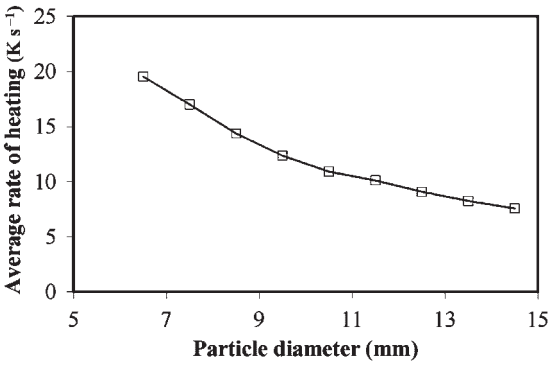

Figure 9. Variation of the average heating rate with particle diameter [41].

As the particle diameter increases, the distance between the particle surface and the center increases. Hence, heat has to travel a longer distance for the larger particles. Therefore, the heating rate decreases with increase in particle diameter.

It can therefore be concluded that the heating rate has a significant role in the devolatilization of coal. Variation of heating rate in a fluidized bed combustor or gasification unit depends on the size of the coal particles. The presence of oxygen enhances the heating rate and hence the oxygen concentration in the fluidizing medium has a significant effect on the heating rate, which is clearly reflected in the devolatilization time of the coal. In addition, secondary reactions in experimental apparatuses cannot be prevented. Therefore, it is not always possible to deduce whether primary or secondary products of pyrolysis have been detected. The contradictory results of some experiments are most often due to the secondary reactions.

2.3.5. Effect of particle size. The influence of particle size on the devolatilization of coal is rather complicated. For the large particles, a number of factors overlap in the devolatilization process. According to Smoot and Smith [42], large particles neither heat rapidly nor uniformly. Therefore, a single temperature cannot be used to characterize the entire particle. The internal char surface provides a site where the secondary reactions occur. The pyrolysis products generated near the center of the particle must migrate outside to escape. During this migration, they may crack, condense, or polymerize, with deposition of some carbon. The amount of carbon deposition increases with the increase in the size of the particle, and hence the yield of volatile matter decreases.

It is not easy to isolate the primary and secondary decomposition reactions for the devolatilization of large particles, because there is a tendency for the secondary reactions to occur within the pore structure. Morris [43] investigated the effect of particle size on the total yield of volatile matter for particles having size in the range of 0.038–2.36 mm. His findings support the fact that the volatile yield decreases with the increase in particle size, which corroborates the findings of Gokhale *et al.* [26]. The study of Morris [43] was performed under mild rates of heating (i.e. 0.34–0.5 K s^{-1} up to 1173 K). The variation in the total yield of various gaseous species with particle size was monitored for a sub-bituminous coal. The results indicate that

there was a slight increase in the yield of tar with increase in the particle size, while the yields of H_2O, CO, CH_4, H_2 and CO_2 decreased. This accounts for the observed decrease in the total yield of volatile matter.

Morris [44] has studied devolatilization under similar reaction conditions for high-rank coals, but at a higher final temperature. He obtained slightly different results. At 1273, 1373, and 1473 K, the yields of methane and hydrogen were found to increase with the increase in particle size. However, the yields of CO and CO_2 were found to decrease with increase in particle size at 1373 and 1473 K, but the same increased with the increase in particle size at 1273 K. This seems to suggest that the effect of particle size is dependent on the temperature and the type of coal, and a transition in the dominating mechanism may occur at $\sim$1273 K for these coals.

Griffin *et al.* [45] have highlighted the effects of particle size on the yield of tar. They used particles having diameter in the range of 0.063–0.075 mm and 0.106–0.125 mm. At the heating rate of 10 K s^{-1}, the tar yield decreased by $\sim$0.5% (by weight) with the increase in particle size (starting from 0.063–0.075 to 0.106–0.125 mm). Higher heating rates (i.e. 1000 K s^{-1} and 2000 K s^{-1}) resulted in corresponding decrease in the tar yield of 3–4 and 5–6% (by weight), respectively.

The large particles induce competition between intraparticle transport and secondary reactions within the pore structure [44]. Griffin *et al.* [45] proposed that the heating rate may modify the effect of particle size via any of the following reasons.

(i) Larger heating rates may increase the driving force for internal mass transfer by intraparticle concentration gradients.
(ii) Changes in heating rate may change the coal morphology and hence the accessibility, surface area, chemical properties of the reactive interfaces, and the characteristic length scales for physical transport. Softening and volatile-generation may temporarily transform the relatively porous coal into a molten material consisting of bubbles, mineral matter, and unsoftened macerals dispersed in liquid continuum, which, before resolidification, may swell into a cenosphere or other shape that is drastically different from the original coal. The resultant effect can be a major decrease in the distance by which the tar must travel to escape the substrate internals.
(iii) The tar yield can vary significantly when the generation and depletion of tar involve significantly different activation energies.

From the foregoing discussion, it can be observed that the particle size studied in most works is less than that used in industrial fluidized beds. The experimental conditions are also not similar to that found in a commercial fluidized bed combustor. In a recent study, Borah *et al.* [16] have reported the devolatilization of coal particles of size in the range of 4–8 mm under fluidized bed conditions in argon atmosphere at a temperature of 1123 K. The velocity of the gas was maintained at 1 m s^{-1}. The ratio of the actual yield of volatile matter to the proximate volatile matter is plotted against the particle diameter in Figure 10. It can be observed from this figure that the yield increased with the increase in particle size. The reason may be that the large coal particles contain large volumes of volatile matter. The distance of travel for the volatile matter may be drastically reduced due to the reason number (ii) given by Griffin *et al.* [45]. Therefore, a large amount of volatile matter can escape through the surface, and hence the yield increases. However, further investigation in this matter is necessary for a more reliable conclusion.

In air and oxygen-enriched air, devolatilization is influenced by the presence of oxygen at the surface of the coal particle. It enhances the rate of heating, which can increase the yield of volatile matter. In addition, if there is any fissure in the coal particle or if the particle fragments, the yield can increase considerably. The results presented by Borah *et al.* [16,46] on the devolatilization of coals of the northeastern India in the presence of air and oxygen-enriched air show that the ratio of the yield of volatile matter to the proximate volatile content of coal did not change significantly with the addition of oxygen to air (see Figure 11), especially for the particles having size between 5 and 9 mm. It is also evident from these works that the additional oxygen in the fluidizing gas did not have any significant effect on this ratio.

Devolatilization time gives the total time required for removal of volatile matter from the coal particle. Tia *et al.* [47] have studied devolatilization in a spouted fluidized bed and reported that flame extinction time increased with increase in particle diameter. The devolatilization time varies with particle diameter

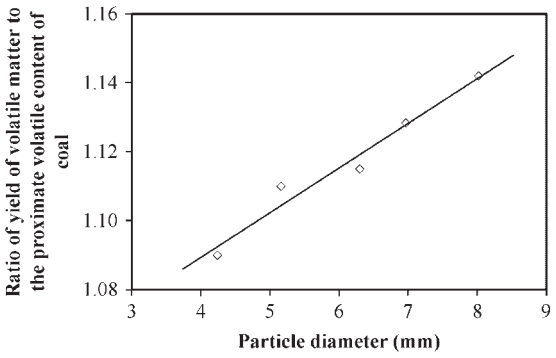

Figure 10. Variation of the ratio of the yield of volatile matter to the proximate volatile content of coal with particle diameter in argon atmosphere [16].

Int. J. Energy Res. 2011; **35**:929–963 © 2011 John Wiley & Sons, Ltd.
DOI: 10.1002/er

obeying the power law correlations given in Tables II and III. The variations for different coals at various fluidization velocities are shown in Figure 12. The increase in devolatilization time with particle diameter is very steep as the particle diameter increases. The correlation parameters vary due to the variations in superficial velocity, experimental apparatus and conditions, particle size, and oxygen concentration.

Borah *et al.* [16,46] have studied the variation of mass of a single coal particle with time under fluidized bed conditions. The coal particle was placed in a basket made of platinum and rhodium net. It was inserted in the freeboard of a hot fluidized bed, and its mass was continuously recorded by a balance which was interfaced with a computer. The variations of mass of coal particle with time in inert atmosphere and air are shown in Figures 13 and 14. They have proposed the following mass versus time correlation for single coal particles.

$$V_a = V_0 + (V_\infty - V_0)[1 - \exp(-Ct^M)], \quad 0 \leqslant t \leqslant t_v$$

where V_a is the mass of coal particle at any time t and V_0 is the initial mass of the particle (i.e. at time $t = 0$). The parameter C in Equation (1) varies with particle diameter and oxygen content of the fluidizing gas. However, M varies with the oxygen content of the fluidizing gas only. The significance of all the parameters of Equation (1) and their correlations are discussed in Sections 2.3.6 and 2.3.7 in details.

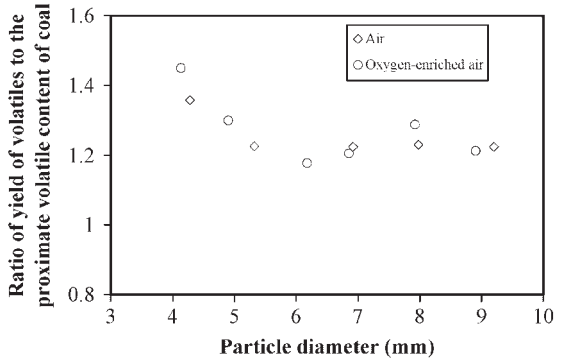

Figure 11. Variation of the ratio of the yield of volatile matter to that of proximate volatile content of coal with particle diameter in air and oxygen-enriched air [16,46].

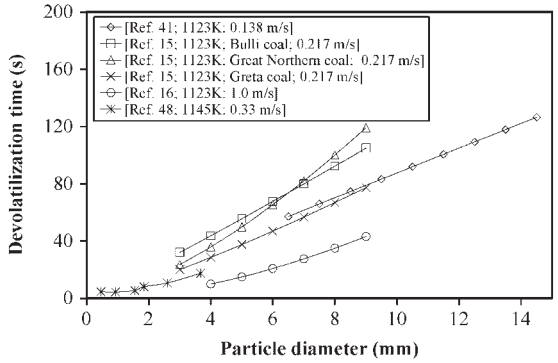

Figure 12. Variation of devolatilization time with particle diameter in inert atmosphere.

Table II. Comparison of devolatilization time at different superficial velocities in inert atmosphere.

		Correlation: $t_v = Ad^n$		
Measurement technique	Superficial velocity ($m\,s^{-1}$)	A ($s\,mm^{-n}$)	n	Temperature (K)
Temperature response [41]	0.138	8.96	0.99	1123
Volatile evolution [48]	0.330	4.15	1.03	1145
Volatile evolution [15]	0.217	9.77	1.08	1123
		4.61	1.48	
		5.18	1.23	
Mass loss measurement [16]	1.000	0.81	1.81	1123

Table III. Comparison of devolatilization time at different superficial velocities in air at 1123 K.

		Correlation: $t_v = A_1 d^{n_1}$	
Measurement technique	Superficial velocity ($m\,s^{-1}$)	A_1 ($s\,mm^{-n_1}$)	n_1
Flame extinction time [17]	0.100	1.84	1.50
Flame extinction time [41]	0.138	1.65	1.52
Flame extinction time [50]	0.312	1.35	1.61
CO_2 profile [49]	N/A	1.48	1.72
Mass loss measurement [16]	1.000	0.55	2.00

2.3.6. Effect of gas velocity. The velocity of the fluidizing gas has an important influence on the devolatilization of coal. It has been reported in the literature [51] that the devolatilization rate increases with increase in superficial velocity. This is very likely due to the greater convective heat transfer as a consequence of the turbulence created by the higher superficial gas velocity. Some of the results reported at different fluidization velocities are shown in Tables II and III. Comparing these results, it can be observed that the devolatilization time decreases with the increase in gas velocity.

In inert atmosphere and air, the parameters of the devolatilization time correlation, $t_v = Ad^n$, vary with the superficial velocity. These are depicted in Figures 15 and 16, respectively. It has been reported in the literature [16] that A diminishes exponentially with the superficial velocity (v) as per the following equation in argon atmosphere.

$$A = 15.08\ \exp(-3.92v), \quad \tilde{R}^2 = 0.99 \qquad (2)$$

where $\tilde{R}$ represents the Pearson correlation coefficient. The parameter n increases with the superficial velocity, which can be described by the following polynomial equation.

$$n = 1.085v^2 - 0.315v + 1.037, \quad \tilde{R}^2 = 0.94 \qquad (3)$$

The coal samples used in these studies are quite different in composition, and the superficial gas velocities employed are quite different in magnitude as well. Therefore, these correlations can be considered as approximate. However, based on the available data, they depict definite trends in the variation of the correlation parameters A and n.

It has been reported in the literature [16] that A_1 exponentially decreases with the increase in the superficial velocity (v) in air, which can be described by the correlation,

$$A_1 = 2.02\exp(-1.24v), \quad \tilde{R}^2 = 0.99 \qquad (4)$$

The parameter n_1 increases with the increase in superficial velocity in air following the correlation,

$$n_1 = -0.0762v^2 + 0.5506v + 1.446, \quad \tilde{R}^2 = 1.00 \qquad (5)$$

Therefore, from the above analysis, it is apparent that the superficial velocity has a significant role on the devolatilization of coal in inert as well as in combustion atmospheres.

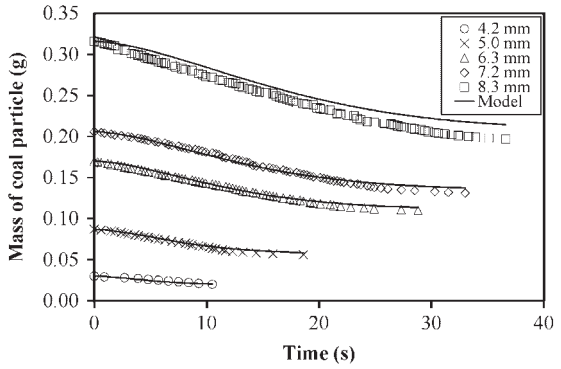

Figure 13. Mass versus time profiles of Baragolai coal in inert atmosphere at 1123 K and 1 m s^{-1} superficial velocity for coal particles of different diameter [16].

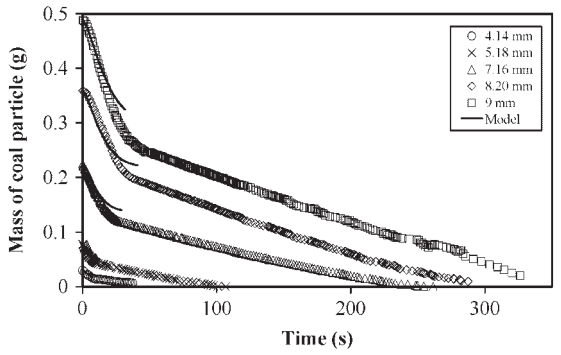

Figure 14. Mass versus time profiles of Baragolai coal in air at 1123 K and 1 m s^{-1} superficial velocity for coal particles of different diameter [16].

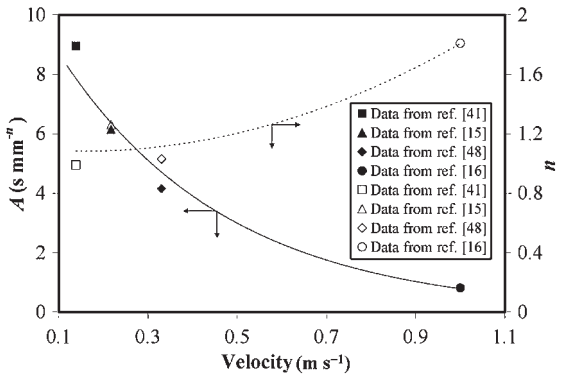

Figure 15. Variation of A and n with superficial velocity in inert atmosphere [16].

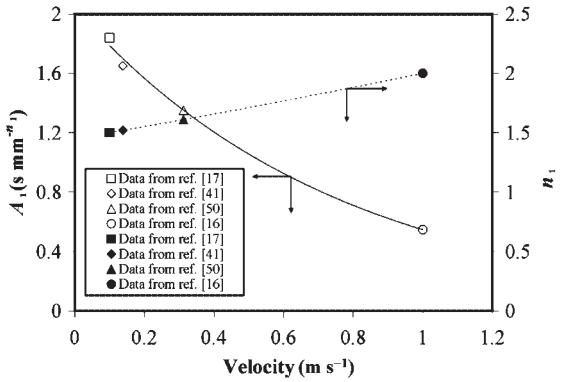

Figure 16. Variation of A_1 and n_1 with superficial velocity in air [16].

Int. J. Energy Res. 2011; **35**:929–963 © 2011 John Wiley & Sons, Ltd.
DOI: 10.1002/er

2.3.7. Effect of volatile content of coal. The amount of volatile matter present in coal has an important influence on its devolatilization. According to Oka [52], the volatile content determined by proximate analysis can be used as a realistic parameter for pulverized coal combustion. However, this is not true for fluidized bed combustion where temperatures and heating rates are lower and the coal particles are much larger. Borah *et al.* [16,46] have reported the yield of devolatilization in three gas atmospheres, viz., inert, air, and oxygen-enriched air under fluidized bed conditions. They have observed an increase in the yield of volatile matter such that the yield becomes greater than the proximate volatile content of coal in all atmospheres. In the inert atmosphere, the average yield was 1.1 times the proximate volatile content of the coal. They have reported that in air and oxygen-enriched air, the total yield of volatile matter decreased with increase in volatile content of coal. Borah *et al.* [16,46] have given separate correlations for these two atmospheres. The total yield of volatile matter can be represented as $\bar{p}$ times the proximate volatile content of the coal, where $\bar{p}$ is the ratio of the total yield of volatile matter to the proximate volatile content of coal. The ratio $\bar{p}$ has a power law correlation with the proximate volatile matter content (V_m) of coal. In air, the correlation can be expressed as follows:

$$\bar{p} = 64.6 V_m^{-1.0974}, \quad \tilde{R}^2 = 0.99 \tag{6}$$

In oxygen-enriched air, the correlation is given by,

$$\bar{p} = 66.315 V_m^{-1.104}, \quad \tilde{R}^2 = 0.70 \tag{7}$$

where V_m is the proximate volatile content of coal. Chen *et al.* [53] have reported similar results during gasification of coal. The volatile content of coal can be enhanced by applying different beneficiation technologies. For example, dry beneficiation technology (such as air dense-medium fluidized bed [54]) can be used to reduce the ash content of coal and increase the volatile content of coal.

2.3.8. Effect of oxygen content of the gaseous medium. Stubington *et al.* [55] have studied the devolatilization of single coal particles having diameter in the range of 1–5 mm in a thermogravimetric apparatus (TGA). The particle was inserted into a furnace, which was already hot, and the flow rate of gas (viz., nitrogen and air) was maintained at $0-100\,cm^3\,min^{-1}$. They observed a decrease in devolatilization time with an increase in temperature and oxygen concentration. This provides evidence that the presence of oxygen in the gaseous medium helps to reduce the devolatilization time.

Because the combustion of volatile matter contributes a large percentage of the total energy evolved during the combustion of a high-volatile coal, it is beneficial if the entire volatile matter evolved from the coal particles burns inside the fluidized bed. However, for large particles, the devolatilization time is longer. Therefore, a major fraction of the volatile matter can burn in the freeboard section. The energy evolved in the freeboard is transferred by convection. Therefore, the high heat transfer coefficient of fluidized bed (which is its major advantage) cannot be utilized appropriately. If the particle size and oxygen concentration are optimized, it may be possible to get a higher heat output (i.e. higher boiler efficiency).

There are very few reports in the literature on devolatilization time in oxygen-enriched air [46,56,57]. A summary of these results is presented in Table IV. It is observed from these results that the devolatilization time decreases with the increase in oxygen concentration. Apparently, the intensity of surface oxidation increases with the increase in oxygen concentration in the fluidizing gas. This increases the rate of heat transfer which increases the rate of release of volatile matter.

Table IV. Correlations for devolatilization time at different oxygen concentrations at 1123 K.

Colliery/coal type	Particle diameter (mm)	Oxygen mole fraction (x_o)	Fluidizing velocity ($m\,s^{-1}$)	Correlation* for t_v (s)
Evans/bituminous [56]	6.7–25.5	0.21	0.3–0.6	$1.31d^{1.6}$
Highvale/bituminous [56]	8.2–34.8	0.01–0.14	0.3–0.7	$0.91d^{1.6}x_o^{-0.086}$
Lignite/lignite [56]	10.2–36.1	0.21	0.3–0.6	$2.36d^{1.26}$
Lingan/bituminous [56]	8.1–33.0	0.21		$1.35d^{1.6}$
	8.1–33.0	0.0–0.14		$1.32d^{1.6}x_o^{-0.029}$
Minto/bituminous [56]	6.0–19.9	0.21	0.3–0.6	$1.29d^{1.6}$
Thorsby/bituminous [57]	9.0–16.3	0.03	0.4	$21.01d^{0.75}$
		0.01		$5.17d^{1.3}$
		0.21		$2.59d^{1.36}$
Bituminous [16]	4.1–9.3	0.00	1.0	$0.81d^{1.81}$
	4.1–9.5	0.21		$0.60d^{1.92}$
Bituminous [46]	4.0–9.3	0.30	1.0	$0.34d^{2.16}$

*x_o represents the mole fraction of oxygen in the fluidizing gas, d represents the diameter of the coal particle, and t_v represents the devolatilization time.

The correlation parameter, C, in Equation (1) can be correlated with the diameter of the coal particle as, $C = A_2 d^{n_2}$. Figure 17 depicts the variation of C with particle diameter in three different gaseous atmospheres. The parameters A_2 varies with the oxygen concentration of the fluidizing gas as described by the polynomial,

$$A_2 = -0.0024(c_{O_2})^2 + 0.2055 c_{O_2} + 3.39, \quad \tilde{R}^2 = 1.00$$

The parameter n_2 varies with the oxygen concentration in the fluidizing gas as described by the following equation:

$$n_2 = \frac{-2.871}{1 + \exp[(c_{O_2} - 37.72)/4.896]}, \quad \tilde{R}^2 = 1.00 \quad (9)$$

where (c_{O_2}) is the concentration of oxygen in the fluidizing gas (expressed as volume percent; Figure 18). The correlation parameter M in Equation (1) can be correlated with the oxygen concentration by the following equation (see Figure 19):

$$M = -0.0008(c_{O_2})^2 + 0.0071 c_{O_2} + 1.6, \quad \tilde{R}^2 = 1.00 \quad (10)$$

The parameters of the correlation, $t_v = A_3 d^{n_3}$, vary with the concentration of oxygen in the fluidizing gas [16]. The constant A_3 varies with the oxygen concentration following a second-order polynomial as shown below [16]:

$$A_3 = -0.0006(c_{O_2})^2 + 0.0032 c_{O_2} + 0.81, \quad \tilde{R}^2 = 1.00$$

The correlation parameter n_3 varies with the oxygen concentration as shown in the following Equation [16]:

$$n_3 = 1.801 + 0.009 \exp(0.1227 c_{O_2}), \quad \tilde{R}^2 = 1.00 \quad (12)$$

The variations of the parameters A_3 and n_3 with oxygen concentration in the fluidizing gas are shown in Figure 20.

2.3.9. Effect of specific heat of coal. The specific heat of coal has a definite relationship with its volatile content [58]. It can be observed from Figure 21 and Table V that the specific heat increases with increase in the volatile content. Specific heat can be a significant factor in the devolatilization of coal because it plays an important role in the rate of heating of coal. Increase in the heating rate induces a more rapid release of the volatile matter. The secondary reactions are reduced

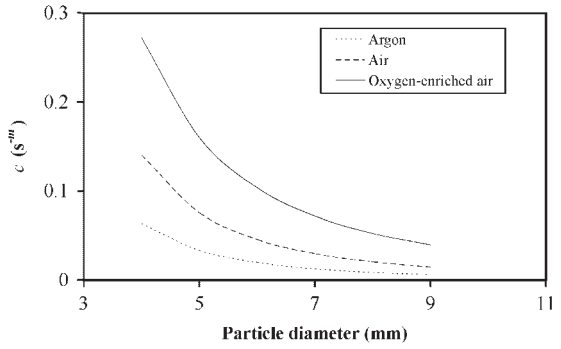

Figure 17. Variation of C with particle diameter in argon, air, and oxygen-enriched air [16,46].

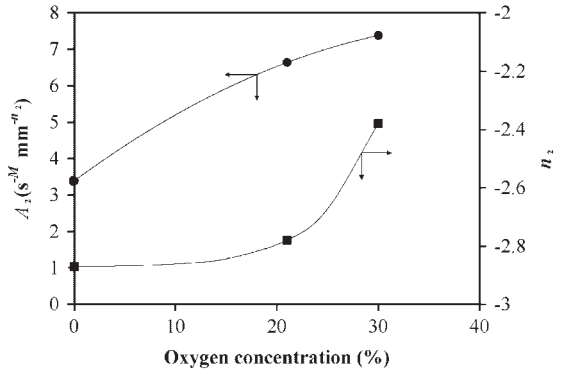

Figure 18. Variations of correlation parameters for constant C with oxygen concentration [16].

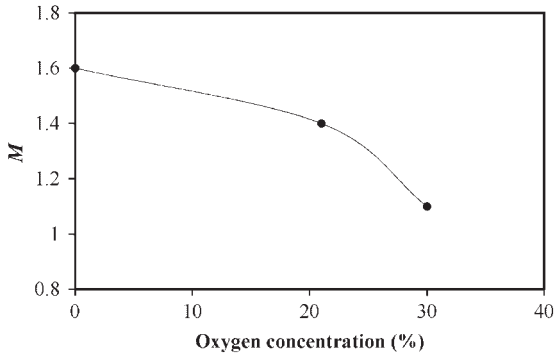

Figure 19. Variation of constant M of Equation (1) with oxygen concentration [16].

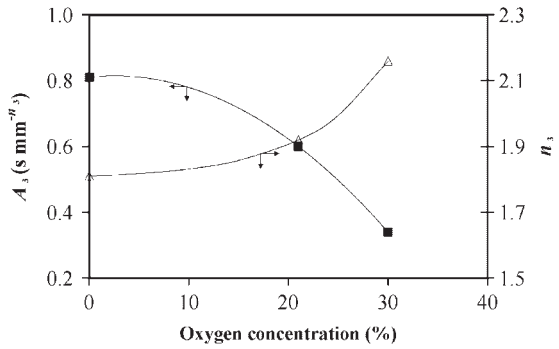

Figure 20. Variations of A_3 and n_3 with oxygen concentration at 1123 K and 1 m s^{-1} superficial velocity [16].

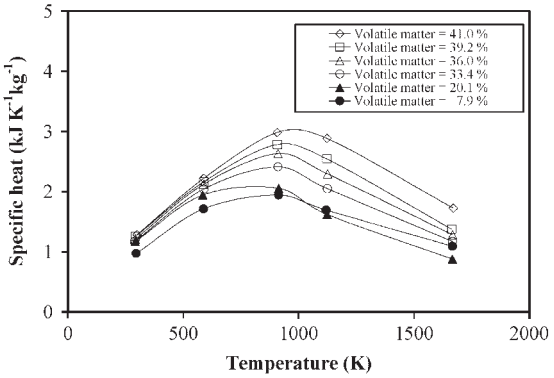

Figure 21. Variation of specific heat of coal with volatile content [58]. The volatile contents reported in the figure are on dry and ash-free basis.

Table V. Analysis (% by weight) of coals studied by Tomeczek and Palugniok [58].

	Raw*	Enriched (by washing)*				
Coal	A_d (%)	A_d (%)	V_{daf} (%)	C_{daf} (%)	H_{daf} (%)	O_{daf} (%)
Czeczot	32.2	3.9	41.0	69.8	4.6	22.9
Boleslaw Smialy	29.1	3.2	39.2	80.5	5.9	11.1
Rydultowy	32.5	7.2	36.0	77.2	4.8	15.1
Wawel	20.1	4.5	33.4	85.2	5.2	7.6
Gliwice	13.0	5.2	20.1	86.6	4.5	4.1
Anthracite	—	4.7	7.9	93.6	3.0	1.0

*A_d, ash content on dry basis; V_{daf}, volatile matter content on dry ash-free basis; C_{daf}, carbon content on dry ash-free basis; H_{daf}, hydrogen content on dry ash-free basis; O_{daf} = oxygen content on dry ash-free basis.

when there is rapid release of volatile matter. This increases the yield of volatile matter beyond the proximate volatile content. There can be variation in the yield of volatile matter during devolatilization depending on the volatile content of the coal. The rapid increase in temperature at the high heating rates reduces the residence time of volatile material [40]. It reduces the effect of cracking of tarry matters inside the particle and hence more tarry liquid is produced. However, the yield of the light hydrocarbon gases remains nearly constant. It has also been reported in the literature [40] that the gain in tar yield with increase in the heating rate is higher for the low-volatile coals than that for the high-volatile coals. This also supports the fact that the low-volatile coals are heated more quickly than the high-volatile coals. Therefore, the residence time of volatile matter is less for the low-volatile coals than that for the high-volatile coals. Therefore, the ratio of the volatile yield to the proximate volatile content diminishes with the increase in the volatile content of the coals.

2.3.10. Effect of fragmentation of coal. Fragmentation is an important parameter in the devolatilization of coal in a fluidized bed. Fragmentation drastically changes the original distribution of particle size in the bed, which affects the devolatilization time of coal particles. Zhang *et al.* [59] have studied the fragmentation of several Chinese coals having different properties in a fluidized bed. The main reason for the fragmentation of coal particles is primary fragmentation, which is caused by the inner pressure (generated by rapid devolatilization) and thermal stress (caused by temperature gradient) within a coal particle. Fragmentation is influenced by the rank of coal, bed temperature, size of the original coal particles, and residence time of the particles in the bed. The volatile matter of coal can drastically influence the degree of the fragmentation of coal particles.

3. IMPLICATIONS OF DEVOLATILIZATION IN FLUIDIZED BED PYROLYSIS, GASIFICATION AND COMBUSTION

A fluidized bed consists of a bed of particles suspended in a gas stream flowing upward at such a velocity that the particles are not carried out of the vessel but continue to circulate vigorously within the vessel. Cavities, called *bubbles*, move through the suspended mass. These facilitate the vigorous circulation of the bed material. Because the bed offers resistance to flow, the drag force, as given by the pressure drop across the bed, is sufficient to support the weight of the bed. The bed has a pseudo-density and has many attributes of a liquid [60]. In combustion applications, fuel is continuously fed to the fluidized bed consisting of non-combustible particles. For solid fuels such as coal, the carbon content of the bed is no more than a few percent. The hot bed particles act as a heat reservoir and stabilize combustion, making the fluidized bed a very desirable device for burning low-grade coals and waste materials.

The bed material consists of coal ash, limestone or sand of $\sim$1 mm diameter. The superficial velocity through the bed is $\sim 2-3\,m\,s^{-1}$ depending on the size of the bed material and the turbulence requirement. The bed temperature is usually kept between 1000 and 1300 K. Lumped coal having a top size of 10–20 mm is fed by a screw or a spreader above the bed. Crushed coal with a top size of $\sim$6 mm is fired pneumatically under the bed. Heat is extracted through the heat exchange surfaces placed within and above the bed. The hot gases leaving the combustor contain considerable

amounts of sensible heat, which can be recovered in various passes through the boiler.

Coal passes through several interactive stages before and during the burning process. These processes are drying (with or without shrinkage), devolatilization (with or without swelling and fragmentation), combustion of volatile matter, combustion of residual char, and attrition of coal particles. Fluidized bed combustion technology offers a flexible method for handling solid fuels of variable quality. One of the advantages of fluidized bed combustion is that large particles can be used, which saves the cost of washing, crushing, drying, and grinding. Fluidized bed combustion can handle coals having high amounts of sulfur and ash, as well as the rejects from the coal washeries.

When a high-volatile coal is introduced into a fluidized bed combustor, the coal particles mix with the bed material, and they start to devolatilize simultaneously [61,62]. Coal particles undergo two overlapping stages of reaction in the fluidized bed, viz., devolatilization and char combustion. The volatile fraction of the coal contributes a significant portion to the total amount of heat released during combustion. The rate of heat released from the volatile combustion is determined by the rate at which the volatile matter can escape from the particles and combine with the oxygen in the gas phase. Therefore, it is important to understand where and how the volatiles are released from the coal. The importance of volatile matter in the fluidized bed combustion of coals has been discussed by La Nauze [60]. Stubington *et al*. [17] noted that the combustion of volatiles in a fluidized bed combustor influences the design and operation via several ways. It affects the distribution of oxygen across the bed, the spacing of the feed points of the coal particles, the split in heat release (and hence the heat transfer between the bed and the freeboard) and the release of nitrous oxide from the bed. Leckner and Lyngfelt [63] have studied the impact of low- or medium-volatile fuels (e.g. coal) and high-volatile fuels (e.g. biomass and waste) on the emissions of NO, N_2O, and other pollutants. It is found that high- and low-volatile fuels behave in different ways. The measures taken to reduce emissions from coal combustion are not necessarily effective for high-volatile fuels. Feng *et al*. [64] investigated the mechanism of N_2O formation, emission of nitrogen oxides (including NO and N_2O) and the effect of the temperature, excess air ratio, and recirculation ratio. The concentrations of nitrous oxide and nitric oxide were measured along the height of the circulating fluidized bed (CFB) furnace. It was found that the N_2O concentration increased with height, and in the exit of the combustor, N_2O concentration reached the highest level. The concentration of NO_x, however, decreased with height, showing the inverse trend shown by N_2O. The emission of N_2O decreased sharply with the increase in temperature at the bottom of the combustor. At the same time, the NO concentration increased.

Stubington *et al*. [55], and Stubington and Linjewile [65] have noted that inefficient in-bed combustion of volatile matter results in undesirably high freeboard temperatures, which facilitates the need for larger heat transfer surfaces in the freeboard region. The evolution of volatiles within the bed is dependent on the mixing of the coal particles [17,66] and progress of devolatilization of the particles from the time of entry to the fluidized bed to the completion of devolatilization. If the progress of devolatilization can be calculated from the time of entry of the coal particles into the fluidized bed, then the total amount of volatile matter present in the bed can be determined at any time. These factors also determine the split between the volatile matter released in the bed and that in the freeboard. Borghi *et al*. [67] noted that the oxygen and temperature profiles in the bed were dependent on the release of volatile matter, because the evolution of concentrated volatile matter in certain regions of the bed can result in areas of oxygen depletion and this can cause hot spots within the bed.

From the foregoing discussion, it is evident that the volatile matter should burn inside the bed so that maximum heat transfer can occur within the bed (which is the main advantage of fluidized bed combustion), and not in the freeboard region. In addition to combustion and heat transfer, evolution of polluting volatile matter from devolatilization is also very important from the environmental perspective. Based on their pilot plant and laboratory scale studies, Borghi *et al*. [67] reported that a major portion of the CO emitted from fluidized bed is related to the release of volatile matter and most of the NO originated from the oxidation of the nitrogenous groups present in the volatile matter. Borah *et al*. [68] have reported the high release of CO in a pilot plant study, which was reduced by the introduction of secondary air for combustion in the freeboard. Atimtay and Varol [69] studied co-combustion of olive oil cake and coal mixture in a bubbling fluidized bed (BFB). They varied the volatile component of the mixture by varying the olive oil proportion in the mixture. They observed that as the volatile component of the mixture increased, the combustion took place more in the freeboard than inside the bed. Furthermore, the CO and hydrocarbon emissions increased as the volatile component increased in the fuel, and the combustion efficiency decreased. Agarwal and Wildegger-Gaissmaier [70] have suggested that the volatile products contribute significantly to the release of CO and NO in the fluidized bed. Stubington and Chan [71] have reported that a definite relationship exists between the volatile matter present in coal and the emission of NO_x. Johnsson [72] emphasized this by stating that the secondary reactions depend on whether the nitrogen is present in the char or present in the volatile matter. García-Labiano *et al*. [73] noted that a large part of the sulfur present in the parent coal is released during devolatilization. The

Int. J. Energy Res. 2011; **35**:929–963 © 2011 John Wiley & Sons, Ltd.
DOI: 10.1002/er

type of sulfur present in the coal and the atmosphere of pyrolysis dictate the type of volatile matter evolved during devolatilization. Much of the chemically bound sulfur is in the form of aliphatic heterocyclic structures containing a thiophene ring system. Memon *et al.* [74] studied the pyrolysis of thiophene. The principal hydrocarbon product at all temperatures was acetylene. Ethanethiol was found to be the major sulfur product together with H_2S formed in significant concentrations at lower temperatures. Carbon disulfide was also formed at higher temperatures. Additional reaction products were CH_4, C_2H_4, C_3H_4, C_4H_3, C_4H_6, C_4H_4, C_6H_6, and C_4H_2. Hence, it is apparent that the optimal design of fluidized bed combustor and the development of pollution control strategy depend on the proper understanding of the mechanism of devolatilization in fluidized bed.

3.1. Devolatilization in inert conditions

Several investigators have studied the devolatilization of large coal particles in inert atmospheres. Zhang *et al.* [50] studied the devolatilization of single coal particles having size in the range of 5–50 mm in a laboratory scale fluidized bed reactor at 1073 K. They employed the minimum fluidization velocity corresponding to 0.5-mm diameter sand particles. Nitrogen was used as the gaseous medium. They concluded that the devolatilization of large coal particles is a strongly non-isothermal process. The total mass-loss during devolatilization differed significantly from the proximate volatile content of the coal. They also observed that the entire volatile matter present in the coal did not release during devolatilization.

Peeler and Poynton [75] studied the devolatilization of single coal particles having size in the range of 1.4–29 mm under simulated fluidized bed conditions at 1173 K in nitrogen atmosphere. The superficial gas velocity was maintained at 0.25 m s^{-1}. They studied nine coal samples ranging from sub-bituminous to semi-anthracite. The devolatilization rate was represented by a reaction order in the range of 0.4–0.6. Stubington and Sumaryono [15] showed that the ratio of yield of devolatilization to the proximate volatile content varied between 0.95 and 1.15 for 3–11 mm diameter coal particles. They studied three Australian coals having volatile matter ranging from 19.4 to 43.5% (by weight) in nitrogen atmosphere at 1023, 1123 and 1223 K. Zhang *et al.* [76] have reported similar results on the yield of volatile matter at 1123 K in a fluidized bed for 5–28 mm diameter Canadian coals. Most of these experimental works have been carried out at the minimum fluidization velocity of the bed material or at a slightly higher velocity. One of the reasons behind this approach may be that the gas velocity was not considered as one of the variables for devolatilization, or only the characteristics during devolatilization were studied. Experimental limitation could be another factor, because the dilution error increases with the increase in gas velocity, and the time-lag or gas-dispersion errors also increase when devolatilization is measured by monitoring the off-gases. Borah *et al.* [16] have reported the ratio of the yield of devolatilization to the proximate volatile content for 4–9.3 mm diameter coal particles having volatile matter in the range of 31 to 41% at 1123 K in argon atmosphere. They employed a superficial gas velocity of 1 m s^{-1}. They observed an increase in the ratio with the increase in the particle diameter. This has been depicted in Figure 10.

From the results reported in the literature, it is evident that the yield of volatile matter is higher than the proximate volatile content of the coal. Therefore, this aspect has to be taken into consideration in the design of a fluidized bed combustor in order to prevent overheating in the freeboard and ensure that the entire volatile matter burns inside the bed. However, the commercial fluidized bed combustors operate at a higher fluidization velocity than that employed in these studies. One of the possible reasons may be that velocity was not considered as one of the variables for devolatilization by these workers. It is also likely that they have only studied the effects of particle size, temperature, and type of coal. In addition, there might be experimental difficulties, e.g. as the velocity is increased, there will be more errors due to dilution, time-lag, or gas dispersion (where devolatilization was measured by monitoring the off-gases). The extent and time of devolatilization depend on the superficial velocity. Therefore, these data on devolatilization need to be extrapolated for the design purpose. Experimental studies on devolatilization need to be performed under the conditions of operation of the commercial fluidized bed combustors.

3.2. Devolatilization in combustion conditions

Saito *et al.* [77] studied the devolatilization of single coal particles of diameter ranging from 2 to 4 mm in combustion atmospheres in a porcelain tube-furnace at temperatures between 1123 and 1373 K. They found that the rate of evolution of volatile matter in air was nearly double of that in nitrogen. In addition, the ultimate loss of mass due to the release of volatile matter was much greater in air than that in nitrogen. The reason suggested by them was that in combustion condition, the coal particle is closely surrounded by a cloud of volatile matter that burns in oxygen. Therefore, the coal particle is additionally heated by the surrounding flame. The resulting higher heating rate causes more release of volatile matter. Stubington *et al.* [55] studied the devolatilization of single coal particles of size in the range of 1–5 mm in a TGA. The particle was inserted into a preheated furnace, and the flow rate of the gas was maintained at 0–100 cm^3 per minute.

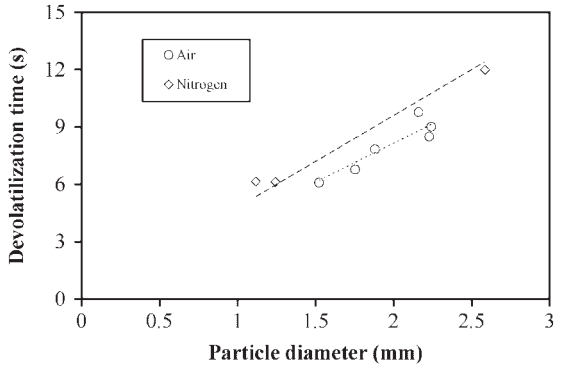

Figure 22. Comparison of devolatilization time in nitrogen and air [55].

Their results show that the devolatilization time decreases with increase in the oxygen concentration (Figure 22).

Winter *et al.* [51] studied the devolatilization and combustion of two sub-bituminous coals in three different laboratory scale fluidized bed combustors. The particle size was 10 mm. The temperature was varied between 973 and 1223 K, the partial pressure of oxygen was varied between 0 and 10 kPa, and the fluidizing velocity was varied from 0.3 to 0.9 $m\,s^{-1}$. They have reported that the release of volatile matter during devolatilization was slightly higher at the higher superficial velocities. In addition, more carbon was lost with the increase in fluidization velocity during devolatilization, and the combustion of char was faster. These observations have been explained by the fact that the convective heat transfer increases with the increase in fluidization velocity. High oxygen concentration slightly increases the ultimate yield of volatile matter as well as the rate of devolatilization due to the high temperature in the flame surrounding the particle. Borah *et al.* [16,46] have reported an increase in the yield of volatile matter in air and oxygen-enriched air. The presence of oxygen enhances the heating rate of the coal particles. The average ratio of the yield of volatile matter to the proximate volatile content has been reported to be 1.25 in air [16] and 1.26 in air containing 30% oxygen [46]. The effect of particle size on the yield of volatile matter may be insignificant if the coal particles fragment, or fissures and cracks develop in the particles. This factor needs consideration in the design of a fluidized bed combustor or gasifier.

3.3. Definition of devolatilization time and the different methods employed for its estimation

The term 'devolatilization' is rather general, which means removal of volatile matter from the coal matrix. No distinction is made regarding the nature of the gaseous surroundings, i.e. whether the atmosphere is inert or oxidizing. Even under oxidizing conditions, pyrolysis-like condition prevails at the initial stage when the devolatilization rate is much higher than the oxidation of the char particle. Hence, this period can be called as devolatilization. The time taken for devolatilization in a fluidized bed combustor is very significant. The devolatilization time must be compared with the particle mixing time in order to decide the appropriateness of the various models proposed for combustion of volatile matter [61]. Most of the workers have inferred devolatilization time from the occurrence of a volatile diffusion flame around the individual particles [78–81]. However, these methods underestimate the total devolatilization time because devolatilization may still occur after the flame has extinguished. Devolatilization time has also been measured from the concentration profiles of the evolved gases [43]. But there exists a time-lag between the volatile evolution and its measurement. Also, the trace amounts of volatile matter, which are evolved during the end of devolatilization, may go undetected due to the dilution affect. Since direct measurements of weight cannot be made if the particle is surrounded by inert particles, thermogravimetric techniques have been applied to the stationary particles [17,70,77]. From these data, the devolatilization time has been defined in different ways, viz., the time for 90% devolatilization [55] or the time for 95% devolatilization [75].

The works reported in the literature on the determination of devolatilization time may be divided into two categories depending on the mobility of the particles in the reactor. In the first category of works, the particles were injected into a hot fluidized bed and allowed to move freely within the bed. Therefore, their immediate environment was similar to the environment in a fluidized bed combustor. In the second category, the particle was dropped into a hot reactor. It either remained stationary in the hot zone on a fixed support, or was suspended in a hot gas stream. Therefore, there were no fluidized particles in contact with the devolatilizing coal particle. In the works belonging to the first category in inert atmosphere, intermittent quenching and removal of coal particles from the bed, and determination of volatile matter have been employed [48]. In this process, devolatilization continues during quenching till its temperature comes down significantly. In air, the flame extinction time was taken into consideration. It is defined as the time counted from the injection of the particle into the bed up to the moment a visible volatile flame is extinguished above the bed. The flame extinction time is possible only at the lower gas velocities. At high gas velocities, the diffusion flame may not be visible. Moreover, the end point may not be visible because the evolution of volatile matter considerably reduces during the end of devolatilization.

Int. J. Energy Res. 2011; **35**:929–963 © 2011 John Wiley & Sons, Ltd.
DOI: 10.1002/er

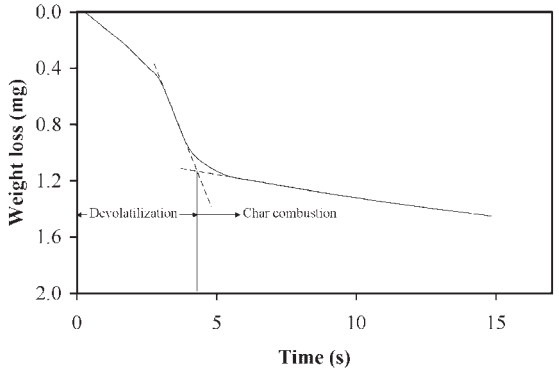

Figure 23. Determination of devolatilization time in presence of oxygen from experimental weight loss profile [55].

Recently, Borah *et al.* [16,46] have measured the loss of mass of a single coal particle under fluidized bed conditions. Both 90 and 95% times were measured in their work. The 95% devolatilization time in inert atmosphere is a reasonable measure because the devolatilization becomes slow toward the end. In the presence of oxygen, devolatilization and char combustion overlap. Therefore, the intersection of the devolatilization and char combustion curves, which is equivalent to 90% devolatilization [55] is appropriate. Figure 23 depicts the determination of devolatilization time in air from the continuous mass-loss profile.

4. MODELS OF COAL DEVOLATILIZATION

There are two types of model that are employed to analyze coal devolatilization, viz., 'structural' and 'empirical' models. The structural models are based on the thermal decomposition process. These models deal with the structure of the parent coal. They require the knowledge of the functional groups present in the coal and their nature. The structural models are generally complex, because they depend on the chemical structure of the parent coal. On the other hand, the empirical models have been extensively developed for both pulverized and large coal particles. An empirical model is generally useful in predicting the rate of volatile evolution and the composition of the devolatilization products for the coals for which it has been developed.

4.1. Structural models of coal devolatilization

Two structural models of devolatilization have been developed, viz., the 'Chemical Percolation Devolatilization (CPD) model' [82–86], and the 'Functional Group- Depolymerization, Vaporization and Cross-linking (FG-DVC) model' [3,87]. The salient features of these models are discussed in the following sections.

4.1.1. CPD model. The CPD model describes the coal conversion behavior based on the chemical structure of the parent coal [82]. This model uses four features of the chemical structure that are directly measured by ^{13}C NMR spectroscopy, viz., (i) the average molecular weight per aromatic cluster, (ii) the average molecular weight per side chain, (iii) the average number of attachments (i.e. side chains and bridges) per cluster, which are referred to as the coordination number, and (iv) the fraction of attachments that are bridges. During devolatilization, the bridges between the aromatic clusters break. These clusters are thermally stable at typical devolatilization temperatures. An unreacted bridge forms a reactive intermediate, which may either cleave to form two side chains or reconnect to form a stable char bridge with release of a part of the bridge as light gas. Reaction rates for this mechanism were obtained by comparison with the measured devolatilization rates. These are independent of the coal (especially at high heating rates). The gas and tar yields are functions of the chemical structure parameters and the reaction scheme. Therefore, they are not input parameters. Percolation lattice statistics are employed to describe the generation of tar precursors of finite size based on the number of cleaved labile bonds in the infinite coal lattice. This is a non-linear relationship, and the percolation lattice statistics provides a closed-form relationship. It avoids the computationally expensive Monte Carlo simulations proposed by Solomon *et al.* [83]. A tree-like structure, called *Bethe lattice*, is used to approximate the coal lattice. The Bethe lattice accounts for the cross-linking present in the parent coal structure. Niksa and Kerstein [84] have used the long-chain approximation.

A generalized vapor pressure correlation for high-molecular-weight hydrocarbons (such as coal tar) has been developed based on the data from coal liquids. The vapor pressures of oligomers are calculated from the temperature and molecular weight at each time step. A flash calculation is performed to determine the fraction of each oligomer that vaporizes at that time step. The vapor–liquid equilibrium mechanism is principally responsible for the variation in tar yield with the change in total pressure in devolatilization experiments. The vapor pressure data of 111 organic compounds existing in coal tar have been presented by Fletcher *et al.* [85]. The cross-linking mechanism permits the reattachment of metaplast (i.e. detached finite fragments) to the infinite char matrix. Since the details of the cross-linking mechanism are poorly known at present, a simple empirical cross-linking rate is employed that is first-order in the amount of metaplast associated with the char.

The coal-independent cross-linking rate is determined by comparison with several sets of data [85].

An improved CPD model incorporating a two dimensional interpolation methodology to compute functional group parameters that are required as input to obtain initial populations of the side chains corresponding to various light gas species has been reported by Jupudi *et al.* [86]. Figure 24 presents a comparison of the predictions by two CPD models with the data for Illinois coal [87].

4.1.2. FG-DVC model. The starting point in the FG-DVC model is the structure of the parent coal, as in the CPD model. However, tar formation and the behavior of the char produced during devolatilization are more extensively treated in this model. In the FG-DVC model, linear oligomers of a certain number of aromatic ring clusters having a molecular weight distribution (characterized by an average and a standard deviation) are linked by a certain number of cross-links per monomer. Cross-links are defined as the points at which more than two attachments connect one cluster to another. During thermal decomposition, bridges are broken and the cross-links are formed. The molecular weight of the resultant oligomers is calculated by randomly distributing these changes [88].

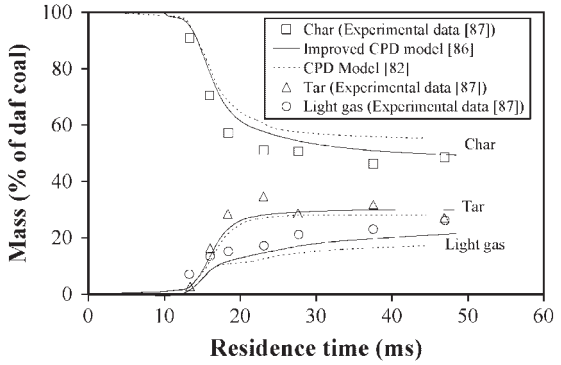

Figure 24. Comparison of the predictions of CPD model and 'improved' CPD model for Illinois (No. 6) coal. The lines represent the model predictions [86].

The devolatilization products as per the FG-DVC and CPD models differ. The CPD model assumes that all molecules, which are not attached to the macromolecular network, are essentially evolved as tars. In the FG-DVC model, it has been assumed that the vapor pressure, which depends on molecular weight, controls whether the molecules are released into the gas phase or not. These gases escape by convective transport from the coal particle. Thus, the tar fraction comprises of aromatic ring clusters, which are released during decomposition. This belongs to the lower molecular weight region with sufficiently high vapor pressure. The remaining fraction is trapped within the coal as either solvent-extractable materials or as liquids. The appropriate mass transport equations have been included in the FG-DVC model.

In the following paragraphs, the application of the FG-DVC model is demonstrated. The model predictions have been compared with the experimental data on the pyrolysis of a Pittsburgh Seam coal [20,87,89,90], a North Dakota (Beulah, Zap) lignite [87,91], and Argonne Premium coal samples [92,93]. Figure 25 compares the predictions from the FG-DVC

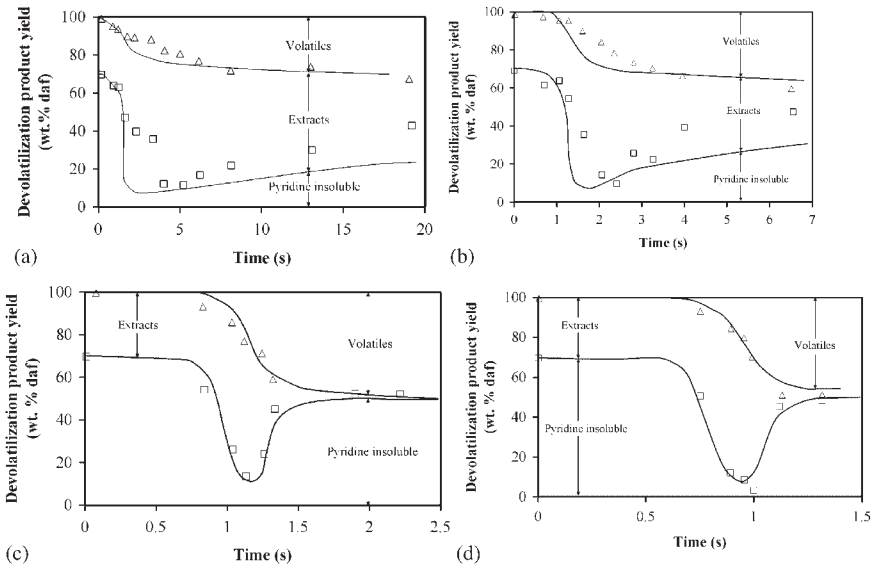

Figure 25. Comparison of the predictions of the FG-DVC model (represented by lines) with the data of Fong *et al.* [90] for Pittsburgh Seam coal at (a) 813 K, 470 K s^{-1}; (b) 858 K, 446 K s^{-1}; (c) 992 K, 514 K s^{-1}, and (d) 1018 K, 640 K s^{-1} [95].

model with the data of Fong *et al*. [90] on total volatile yield and extract yield as a function of temperature. The pyrolysis was carried out at 86 kPa [94]. The experiments were performed in a heated-grid apparatus at the heating rate of $\sim 500\,K\,s^{-1}$ with variable holding times and provisions for rapid cool down. There is a slight discrepancy between the prediction and the data at early times at the lower temperatures (Figure 25(a) and (b)). The predictions at the higher temperatures (Figure 25(c) and (d)) are in excellent agreement with the data. It is possible that the coal particles are heated at a slower rate than the nominal temperatures given by Fong *et al*. [90], which could be the reason behind the slight mismatch.

To examine the effect of the rank of coal on cross-linking, the volumetric swelling ratios (VSR) for North Dakota (Beulah, Zap) lignite and Pittsburgh Seam bituminous coal were measured as a function of temperature at a heating rate of $0.5\,K\,s^{-1}$. The VSR can be related to the cross-link density [89,95]. It has been reported in the literature [83,91] that the cross-linking reactions may also release gaseous species. Under this assumption, the VSR was correlated with the gaseous species evolved during pyrolysis. Correlations presented in literature [83,91] show that the evolution of CO_2 from lignite and CH_4 from bituminous coal appear to have similar effects on the VSR. Reactions that form these gases leave behind free radicals, which can be stabilized by cross-linking. The coals, which undergo early cross-linking, are less fluid, produce less tar (of lower molecular weight) as compared with the coals which do not experience early cross-linking [96]. Based on the assumption that a cross-link is formed for each CO_2 or CH_4 evolved from the char, the predictions from the FG-DVC model are in good agreement with the data [83,91].

A sensitive test of the FG-DVC model is its ability to predict the molecular weight distribution of tar, and its variation with the rank, pressure, and heating rate. The predictions are compared with the experimental results for the Pittsburgh Seam bituminous coal and Beulah Zap lignite pyrolyzed in the field ionization mass spectrometer (FIMS) apparatus [97]. The data were summed over 50 amu intervals. Although the Pittsburgh Seam bituminous coal showed peak intensity at ~ 400 amu, the lignite peak appeared at ~ 100 amu. The predicted average tar molecular weight distributions are in good agreement with FIMS data, as shown in Figure 26(a) and (b). Note that one data point represents the average intensity over 50 amu intervals in these figures. Since both tar distributions are from the same monomer distribution, the enhanced drop-off in amplitude with increased molecular weight for lignite, as compared with bituminous coal, must be due to early cross-linking and transport effects in the lignite.

The FG-DVC model can also predict the effect of pressure on the tar molecular weight distribution and product yield [83]. The internal transport rate is inversely proportional to the ambient pressure. The reduced transport rate reduces the evolution rate of the heavier molecules. Therefore, the average molecular weight and the vaporization 'cut-off' decrease with increase in the pressure. This model was able to successfully predict variations in the tar and char yields from pyrolysis experiments executed over a range of pressures (i.e. from vacuum to ~ 10 MPa) [83].

A parity plot of predicted versus measured tar yields at atmospheric pressure is shown in Figure 27. A perfect agreement between the model prediction and experimental data corresponds to the diagonal line in

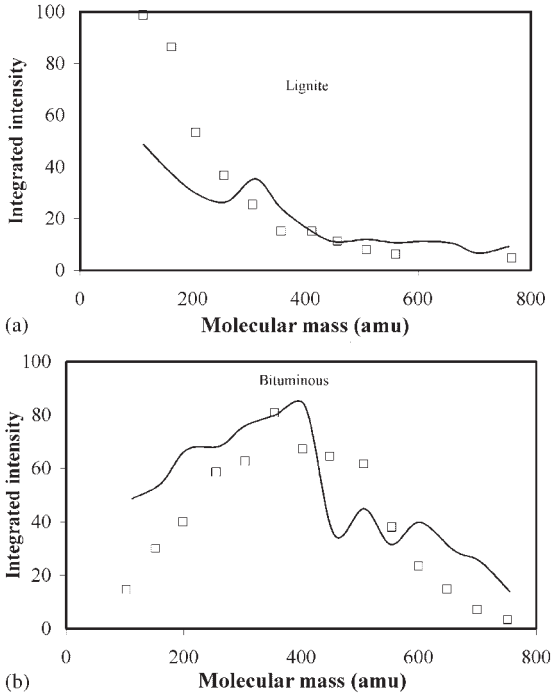

Figure 26. Comparison of predicted and measured tar molecular weight distributions for lignite and bituminous coals [97].

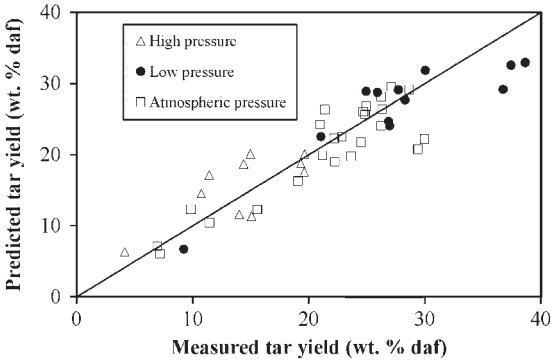

Figure 27. Comparison of the measured and the predicted tar yields for a number of coals [98].

the figure. The experimental data shown in Figure 27 constitute different experimental set-ups and conditions. It is observed that all the data indeed fall on or near the diagonal. Some other examples of the agreement between the model prediction and experimental data are shown in Figures 28–30.

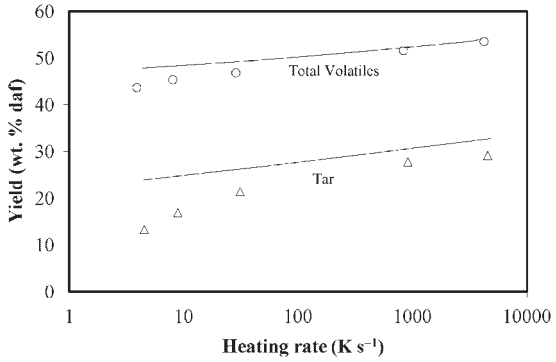

Figure 28. Variations of tar and total volatile yields with heating rate at atmospheric pressure for an Illinois coal. The predictions are shown by the solid lines [98].

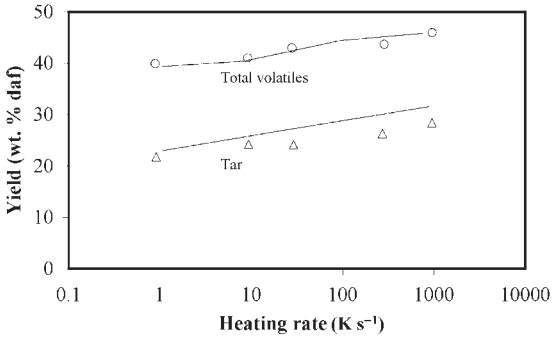

Figure 29. Variations of tar and total volatile yields with heating rate at atmospheric pressure for a Linby coal. The predictions are shown by the solid lines [98].

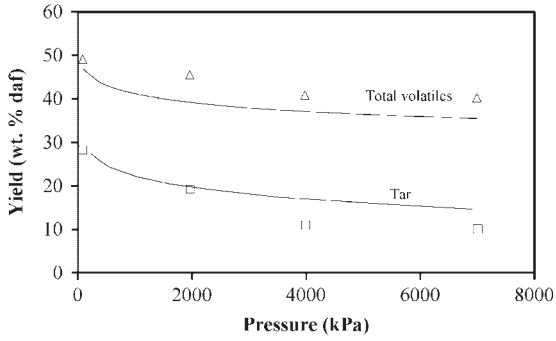

Figure 30. Variations of tar and total volatile yields with pressure at 1000 K s^{-1} for an Illinois coal. The predictions are shown by the solid lines [98].

4.1.3. Advantages and disadvantages of structural models. Structural models such as the CPD and FG-DVC are useful in predicting the production of tar and char, and evolution of light gases during the devolatilization of coal [3,4,82–86,88]. The FG-DVC model is able to predict behavior such as cross-linking, hydrogen utilization, and fragmentation during devolatilization [3,4,88]. It can also predict the swelling and solubility of coals, and can distinguish between the evolved tar and solvent-extractable liquid products generated during devolatilization with reasonable accuracy [3,4,88]. Both of these models utilize the data generated by instrumental analysis. The quality of data must be high and these are highly coal specific. This restricts the scope of the model to a unique type of coal, which corresponds to the input data. The major success of these models is in the prediction of the variation of yields of tar and char with operating conditions. This is achieved because these models consider the structural aspects of coal. With the inclusion of mass transfer aspects, the FG-DVC model has become more complex. The CPD model is computationally more efficient than the FG-DVC model in its treatment of coal structure [88], and it is also somewhat less complex.

4.2. Empirical models of coal devolatilization

Empirical models adopt a less sophisticated approach than the structural models. They take a global approach to the modeling of devolatilization. Empirical models were originally developed to model the devolatilization of pulverized bituminous coals. A general discussion on the empirical modeling approach is given in the following sections.

4.2.1. Single first-order Arrhenius models. Since the complex chemical reactions and transport processes occurring within the coal particle are not well understood, a number of simple first-order Arrhenius-type models have been developed. Such models have been used by van Krevelen *et al*. [99], Stone *et al*. [100], Howard and Essenhigh [101], Wiser *et al*. [102], Badzioch and Hawksley [103], Anthony *et al*. [37], Kobayashi *et al*. [104], Maloney and Jenkins [105], Niksa *et al*. [29], Sandhu and Hashemi [106], Gokhale *et al*. [26], Fu *et al*. [107], and Sharma *et al*. [108] for coals as diverse as bituminous and brown types. The general form of the model can be represented by the following equation:

$$\frac{dV}{dt} = k(V^* - V) \tag{13}$$

where V^* is the ultimate yield of volatile matter, and $V \to V^*$ as $t \to \infty$. The kinetic rate constant, k, varies with temperature following the Arrhenius equation,

$$k = k_0 \exp(-E/RT) \tag{14}$$

Experimental support for these models has been presented in a number of works [26,29,37,99–108]. The

Int. J. Energy Res. 2011; **35**:929–963 © 2011 John Wiley & Sons, Ltd.
DOI: 10.1002/er

kinetic parameters of these models are extremely sensitive to the operating conditions, and they vary significantly to produce a reasonably good fit. These models are applicable where the kinetic parameters have been evaluated using the experimental data.

4.2.2. Models with m*th-order kinetics*. The *m*th-order reaction models use the following devolatilization equation.

$$\frac{dV}{dt} = k(V^* - V)^m \tag{15}$$

According to Peeler and Poynton [75], the *m*th-order kinetic model is extremely useful in predicting the mass-loss data for particles in the size range of 1.4–29 mm, and coals ranging from sub-bituminous to semi-anthracite types. Their data were recorded by suspending the coal particle from a microbalance into a hot stream of nitrogen gas, and the transient weight loss profiles were analyzed. The experiments were conducted at 1173 K and the rate constant, k, was related to the particle size as,

$$k = p\hat{d}^q \tag{16}$$

where $\hat{d}$ is the geometric mean diameter of coal particle, and p and q are coal-dependent parameters. The reaction order was reported to vary between $m = 0.4$ and 0.6 depending upon the type of coal [75].

The reaction rate constant is found by choosing the reaction order so that fractional devolatilization varies linearly with time. Peeler and Poynton [75] have shown that the rate expression fits the experimental data well. They have given a linear relationship between devolatilization time and particle diameter, which is shown in Figure 31. The reason for some deviation observed between the fit of the model and the experimental data may be that the experimental temperature (1223 K) was higher than the temperature employed by Peeler and Poynton (i.e. 1173 K) [75].

In contrast to the reaction orders reported by Peeler and Poynton [75], Li *et al*. [109] have reported reaction orders between $m = 1.27$ and 4.5. The particles studied by them were small (viz., −0.125 and +0.075 mm). They used a TGA with a variable heating rate. The lower reaction orders indicate that the devolatilization of large coal particles becomes less kinetically controlled as the particle size increases, and phenomena such as heat and mass transfer become increasingly important.

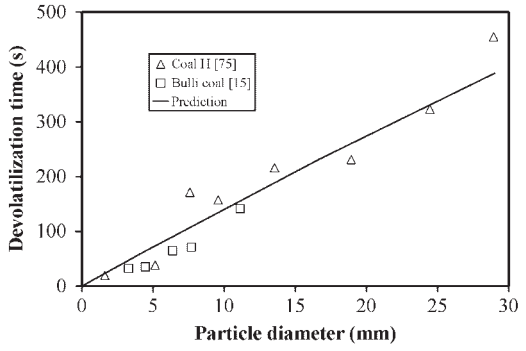

Figure 31. Variation of devolatilization time with initial particle size [75].

4.2.3. Competing reaction models. The inability of the single first-order and *m*th-order reaction models to describe the devolatilization behavior of coals over a wide range of operating conditions has led to the development of more sophisticated reaction models such as the 'competing reaction' models. Doolan *et al*. [110] combined the single first-order model for volatile evolution with a similar term describing the decomposition of volatile matter according to the following equation:

$$\frac{dV_i}{dt} = k_{vi}(V_i^* - V_i) - k_{di}V_i \tag{17}$$

where V_i represents the yield of species i and V_i^* represents the ultimate yield of the same species. k_{vi} denotes the rate of evolution of species i, which is proportional to the amount of species i remaining in the coal, i.e. $(V_i^* - V_i)$. k_{di} refers to the rate of decomposition of species i, which is related to the amount of species i which formed V_i. A similar approach was used by Cliff *et al*. [22], and Yang and Wang [111]. Jamaluddin *et al*. [112] have compared the effectiveness of several models. They have reported that the competing reaction model was able to provide better predictions over a range of heating rates. It predicted the final temperature more accurately than the single first-order reaction model. It also performed better in predicting the yields of various volatile species at the higher temperatures.

4.2.4. Multiple parallel reaction models. In multiple parallel reaction models, a particular volatile species is evolved via a number of simultaneous, independent, first-order reactions. Each species is derived from a number of sources within the coal structure, each of which yields the species according to differing kinetics. Tomeczek and Kowol [113] proposed that individual volatiles can be derived via several (usually four to six) simultaneous, independent, first-order reactions. Several models have been developed in which coal devolatilization has been described by infinite number of simultaneous, independent, first-order reactions [31,59,114–123]. A significant amount of work has been carried out using the multiple parallel reaction models for large particles. Agarwal *et al*. [114] concluded that the modeling approach involving multiple parallel reactions was able to predict both mass-loss and evolution of individual gaseous species from large coal particles with reasonable accuracy.

However, as the time increases, the computational time necessary for calculating the volatile yield becomes increasingly larger.

4.2.5. Shrinking-core model. It has been demonstrated in the literature [124] that the devolatilization of coal can be described by the shrinking-core model, assuming no change in the size of the particles. Chern and Hayhurst [124] performed devolatilization studies with bituminous and lignite coals in a fluidized bed in nitrogen atmosphere by withdrawing coal particles from the hot bed before any fragmentation could occur. The particle was then quenched in nitrogen, weighed, sectioned, and examined under a microscope. Apart from the final stages of devolatilization, these particles had a central core of virgin coal, surrounded by char. The boundary between these two regions was sharp, indicating a shrinking core. The velocity of the movement of the boundary was found to be constant. This conclusion was confirmed by the measurement of the mass of the particle with time. They developed a model incorporating heat transfer from the fluidized bed to the exterior of the coal particle, followed by heat conduction through the outer layer of the char to provide the enthalpy required for the endothermic thermal decomposition in the moving reaction zone. This model predicts that apart from the very beginning and the end of devolatilization, there is an almost constant velocity of the shrinking core of the raw coal. They concluded that it is possible to describe the generation of volatile matter with a simple shrinking-core model, at least for the early stages of pyrolysis. They also concluded that although their model matched and described the observations well for bituminous and lignite coals, it was not suitable for anthracite coals, which chatter into many pieces soon after entering the hot fluidized bed. The time for devolatilization, t_v, is given by,

$$t_v = \left(\frac{\rho \Delta H}{k_t \Delta T}\right)\left(\frac{k_t}{3ah} + \frac{1}{6}\right)a^2 \tag{18}$$

where k_t is the thermal conductivity of coal, a is the radius of the coal particle, h is the convective heat transfer coefficient, ρ is the density of original coal, ΔH is the enthalpy required to devolatilize unit mass of coal, and ΔT is the difference of temperature between the fluidized bed and the surface of the shrinking reaction core.

This model is based on several assumptions. As mentioned earlier, it assumes that devolatilization proceeds with a shrinking core of virgin coal surrounded by char. Because of its relatively high porosity, the char offers no resistance to the gases and vapors leaving the thin reaction zone. Devolatilization is controlled by the rate at which the enthalpy for thermal decomposition is provided by convective heat transfer from the bed to the outer surface of the particles and subsequently by conduction through the char.

Equation (18) shows that if h is finite, the effect of external heat transfer is to prolong devolatilization time by a factor $[1+2k_t/(ah)]$ over the case when $h = \infty$. Chern and Hayhurst [124] derived the following equation for devolatilization time.

$$t_v = \frac{t\left(\frac{k_t}{ah} + \frac{1}{2}\right)}{\frac{k_t}{ah} - \frac{3}{2}\left(\frac{r_c}{a}\right)^2 + \left(1 - \frac{k_t}{ah}\right)\left(\frac{r_c}{a}\right)^3 + \frac{1}{2}} \tag{19}$$

They have plotted the calculated values of r_c/a (where r_c is the radius of the shrinking core) calculated from Equation (19), against t/t_v (where t is the time) for values of $k_t/(ah)$ ranging from 0 to 25. Although Equation (19) is a cubic equation, there are regions for $0.1 < k_t/(ah) < 5$ where the plots are actually straight lines. They showed that for $k_t/(ah) = 0.5$, there is a prolonged linearity. The quantity, $k_t/(ah)$, is a measure of the relative magnitudes of the convective and conductive resistances, which is often expressed in terms of the Biot number (defined as, $B_i = ha/3k_t$).

Chern and Hayhurst [124] have stressed upon the excessive simplicity of the steady-state treatment of their model. In their model, the coal decomposition temperature was assumed to be constant, which is not true for the low-rank coals, which decompose at a lower temperature. The thermal conductivity was assumed to be independent of temperature, which is also not accurate. The particle radius was assumed to be constant, which is questionable as particles undergo swelling and develop fissures in the char. All the sensible heat for coal and char was assumed to be negligible as compared with the enthalpy of devolatilization. Loss of moisture from the coal and the associated latent heat were ignored. Intrinsic kinetics of devolatilization was assumed to be very fast. Chern and Hayhurst [124] arrived at the conclusion that despite all these simplifications, the shrinking-core model predicts that at least during some parts of devolatilization, there is constant velocity at which the core of the raw coal shrinks.

4.2.6. Advantages and disadvantages of the empirical models. The simplicity of the empirical coal devolatilization models is due to the assumption that the entire process can be represented by a simplified overall reaction rate on a global scale, rather than consideration of the rupture of individual bonds within the coal macromolecule. The second advantage is that extensive data related to the structure of the coal are not required in these models. The data necessary to supplement the empirical models can be obtained with far simpler techniques than that required for the structural models (mainly due to the type of data involved).

Empirical models have no distinct relation with the parent coal structure, which is a limitation for rigorous modeling of devolatilization. Other coal properties

Int. J. Energy Res. 2011; **35**:929–963 © 2011 John Wiley & Sons, Ltd.
DOI: 10.1002/er

related to the structural changes occurring during devolatilization (e.g. solvent swelling) cannot be predicted by these models. Empirical models are less effective in predicting the yields of tar, char, and volatile gases. Empirical models are deterministic by nature. They use the average values of the fluctuations of parameters, which are determined experimentally. Hence, the empirical models are useful only within the range of data, which are used for the development of the model.

5. MODELING OF DEVOLATILIZATION OF LARGE COAL PARTICLES

Modeling of devolatilization of large coal particles differs from that of the pulverized coal particles, because the temperature of the particle can no longer be assumed to be uniform throughout the particle during heating (i.e. lumped approach). This is particularly relevant in fluidized bed systems where high heat transfer rates deliver heat rapidly to the particle surface. Longer devolatilization time may result due to the internal heat conduction limitations, which result in a slower transfer of heat to the center of the particle.

5.1. Kinetic modeling

The most significant change in the devolatilization mechanism for large particles (which are relevant to fluidized bed pyrolysis) is due to the secondary devolatilization reactions. During this stage, the primary volatiles undergo cracking, condensation, polymerization, and char formation reactions while transported out of the particle. The FG-DVC model for coal devolatilization is the most comprehensive structural model which incorporates the transport processes into the overall model. However, it has a major limitation because of its inherent complexity. Empirical models present a less complicated solution and therefore, these models may be suitable for integration into the devolatilization models for large particles. This has been performed in several studies [18,73,75,107,113–116,118,121,125]. These studies have shown reasonable success in predicting the total mass-loss and evolution of individual volatile species from the large coal particles during devolatilization. However, the predictions of empirical models are limited to the experimental condition, experimental set-up, particle size, and coal properties.

Peeler and Poynton [75] have determined the kinetic parameters for various types of coal by fitting the experimental data of devolatilization. They found the order of the reaction by trial and error, and determined the reaction rate constants. The reaction rate constant was found to depend on the properties of coal. Once the reaction order and the rate constant are known, the mass-loss profiles of large coal particles with time can be predicted. Peeler and Poynton [75] have verified their model with the data of Stubington and Sumaryono [15] (Figure 31). In this model, the data on coal structure or information on bond linkage are not necessary. This model, however, does not give any information on the production of tar and gas during devolatilization.

5.2. Modeling of heat transfer

Large internal temperature gradients during the heating of large coal particles have been reported by García-Labiano *et al.* [73], Tomeczek and Kowol [113], Agarwal *et al.* [115], and Adesanya and Pham [121]. Tomeczek and Kowol [113] highlighted the importance of particle temperature response by stating that any verification of model by mass-loss data alone is not sufficient, and the model should be verified by means of the predicted and measured temperature responses.

Zedtwitz *et al.* [126] developed a numerical model for heat transfer for steam gasification of coal in a fluidized bed contained in a quartz tubular reactor that was directly exposed to concentrated thermal radiation. The Monte Carlo method was applied for solving the radiative exchange within the reactor walls, bed particles, and the gas phase. The reaction kinetics was described by Langmuir–Hinshelwood type rate laws. After comparing experimentally measured values with the numerically computed temperature profiles, product gas compositions and conversions, they concluded that heat is transferred to the particles predominantly by thermal radiation and to the gas by particle–gas convection because absorption of radiation by the particles is three orders of magnitude higher than that of the gas phase.

5.3. Modeling of mass transfer

It is generally acknowledged that mass transfer of volatile products within the particle is a significant factor in coal devolatilization [15,59,113,114]. The role of mass transfer during devolatilization cannot be ignored especially for the large coal particles, because the volatile mass produced must go out through the particle surface. Many factors such as ambient pressure, pore size, and volatile content can influence the transport of volatiles.

Winter *et al.* [51] have studied the devolatilization of coal at fluidization velocities in the range of 0.3–9 $m\,s^{-1}$. They reported that with increase in the fluidization velocity, the loss of carbon during devolatilization increased. This was attributed to the higher rate of transfer of oxygen to the surface of the particle. Relatively few studies on mass transfer in the devolatilization of large particles have been reported. Peters and Bertling [30] studied the pyrolysis of coking coals in the size range of 1–15 mm. They pointed out that larger temperature gradients could exist within the particle for

high external heat transfer coefficient (as would be encountered in fluidized beds). They interpreted their results by comparing the devolatilization process to the drying of coke. They developed a correlation of fractional release of volatile matter with the temperature of pyrolysis and particle size, which is given by the following equation:

$$\frac{V}{V^*} = 3 \times 10^{-4}(T_b - 330)d^{-0.26}t \tag{20}$$

where T_b is the temperature of the fluidized bed, d is the particle diameter, t is time, V is the volatile matter evolved at time t, and V^* is the total volatile matter evolved. Essenhigh [78] studied the devolatilization of particles having diameter in the range of 0.295–4.76 mm in a non-fluidized combustion system. According to his model, the volatiles form a drop and the volatile matter transfers from the drop surface to the outside. Assuming mass transfer as the rate-limiting step, he proposed that the time required for devolatilization could be predicted by the following equation:

$$t_v = \sigma_d\left(\frac{\eta}{8Pc_a}\right)\left(\frac{V^*}{100}\right)d^2 \tag{21}$$

where P is the permeability of the char, η is the viscosity of the flowing volatile matter, σ_d is the density of the drop liquid, and c_a is the proportionality constant between the rate of transformation of liquid to vapor at the surface of the drop (per unit area) and the rate of shrinkage of the drop.

La Nauze [60] has proposed a model for devolatilization assuming internal mass transfer as the rate-controlling step. The total time for volatile evolution was shown to follow the equation,

$$t_v = \frac{\rho_v d^2}{24Dc} \tag{22}$$

where ρ_v is the molar density of volatile matter in the particle, D is the effective diffusivity of the volatiles through the char of diameter d, and c is the mean value of concentration of volatiles, assuming a uniform distribution of potential volatile species throughout the particle. The approach of LaNauze [60] is similar to that of Essenhigh [78], except in the treatment of the diffusion process. Gavalas [38] has studied the effect of mass transfer limitation on the pyrolysis of coal. Jüntgen and van Heek [127] have presented two different models that take into account the transition from reaction-controlled pyrolysis (independent of particle size) to diffusion or heat transfer-controlled pyrolysis (dependent on particle size and rate of heating). They suggested that under the conditions of fluidized bed combustion, where the rate of heating is $\sim$20–170 K s^{-1}, the process is reaction-controlled when the particle diameter is $<$0.6 mm.

6. ECONOMIC ANALYSIS

Koornneef *et al*. [128] have analyzed the development and economical performance of FBC boilers. They have prepared a database of technological and economic data on nearly 500 FBC projects. Analysis of these projects shows that the variants of FBC, viz., CFB and BFB, technologies have evolved differently over time. Market regulation, environmental legislation, and R&D programs are the key parameters for the market acceptance and technological development of FBC. The important driving forces for FBC technology are fuel availability, required applications in the market, innovation spill-over and competing technologies. There are continuous improvements in fuel diversification, technical availability, efficiency, and emissions. Koornneef *et al*. [128] have observed that there is a decline in specific investment cost in terms of economical performance. The effect of technological learning and experience on the economic performance of FBC technology was analyzed using the experience curve method and the theory of economies of scale.

6.1. Experience curve

One way of measuring technological learning or experience is by the economical performance of the technology. The International Energy Agency states that price is the most important measure of performance in a new technology [129]. The measurement of learning and experience can be a useful tool to analyze the trend of cost reduction of new energy technologies. Experience curve depicts the learning in terms of everyday experience and the activities of the engineers, sales representatives, and other employees. According to Lundvall [130], it can be summarized under three types of learning, viz., learning by doing (i.e. increasing the efficiency of production operations), learning by using (i.e. increasing the operation efficiency of complex systems), and learning by interacting (i.e. by the interaction between users and producers).

By analyzing these trends, prospects of future energy cost, potential and commercialization of a new energy technology can be made [131]. A well-established and documented method for quantifying technological change with the use of economical factors as measuring tool is the experience curve. The general equation of experience curve is expressed as [131]:

$$C_{cum} = C_0(N_{cum})^b \tag{23}$$

where C_{cum} is the cost of a unit after a number of cumulative units are produced, C_0 represents the cost of the first unit, and N_{cum} is the cumulative number of units produced. The most important element in this equation is the experience index, b. It is the slope of the curve of the cumulative production of FBC units versus the EPC prices, as depicted in Figure 32. It defines

Int. J. Energy Res. 2011; **35**:929–963 © 2011 John Wiley & Sons, Ltd.
DOI: 10.1002/er

the steepness of the curve and thus determines the reduction of cost. The index b can be calculated for every doubling of the cumulative production. The quantity $(1–2^b)$ is called the *learning rate* (LR) and 2^b is the *progress ratio* (PR). The progress ratio quantifies the relationship between cumulative production and cost (or price). A progress ratio of 0.9 means that the cost to produce a unit after one doubling of cumulative production is 90% of that of the first unit produced. Experience curves are mainly expressed in logarithmic axes. When plotting in logarithmic axes, equal relative changes in ordinate and abscissa are expressed linear. The main advantage of this method is that the line (i.e. the experience curve) appears in the form of a linear equation. Hence, the decline of cost can easily be observed and compared with other technologies. The experience curve can be developed by regression analysis. The analysis also yields two valuable indicators for the 'quality' of the estimated relationship. The value of $\tilde{R}^2$ indicates the goodness of the fit of the model. Figure 32 depicts the experience curve for EPC (i.e. engineering, procurement and construction) prices of new CFB plants in North America for no fuel challenge and standard design.

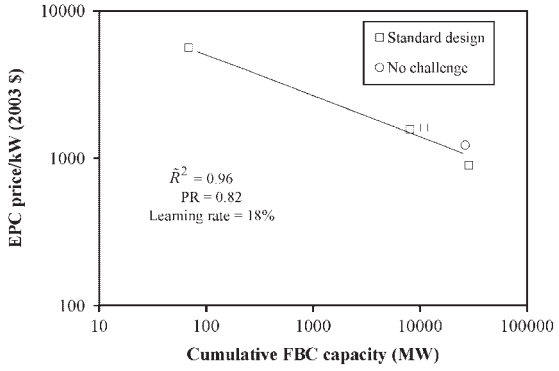

Figure 32. Experience curve for EPC prices of a new CFB plant in North America for no fuel challenge (e.g. polyethylene, plastics and wood bark) and standard design (i.e. coal) [128].

The analysis by Koornneef *et al.* [128] yielded progress ratios (PR) ranging from 0.42 to 0.93 for different groups of projects (e.g. new plant, repower (i.e. repowering of existing power plant with new equipment and modification), retrofit, add-on and conversion) and different parts of the capital breakdown (e.g. total project price, EPC price, and boiler price). This means that the specific investment prices decline with every doubling of the cumulative installed capacity. The progress ratio for new FBC plants lies between 0.90 and 0.93. These values correspond with the average PR of 0.9 for power plants reported in the literature [128]. The economies of scale (scale-up) have a significant influence on the investment price. Scale factors are found in the range of 0.62−0.81 for different groups of projects. According to these scale factors, specific investment price decreases, respectively, between 25 and 12%, with every doubling of the plant capacity.

Borah *et al.* [46] have presented approximate capital cost of an atmospheric fluidized bed combustor (AFBC) with air containing 30% oxygen, which was calculated using the data reported by M/S Alstom Power Inc. [132]. The unit costs were compared with the data given by Wong and Whittingham [133]. These are presented in Table VI. From this table, it can be observed that the unit cost of the AFBC system is lowest. When an AFBC is upgraded with additional requirement of oxygen, the unit cost becomes higher than the subcritical and supercritical pulverized coal combustion systems as well as the atmospheric fluidized bed combustion system. However, the cost is still lower than the pressurized fluidized bed combustion system and IGCC. Since the devolatilization time in oxygen-enriched air is shorter in comparison with air [46], the combustion efficiency and boiler efficiency are likely to be higher than that in the AFBC. The plant efficiency is anticipated to be marginally lower than the AFBC because of the consumption of power for air separation. A comparative study of CO_2, SO_2, NO_x, and particulate emission has also been presented in Table VI.

Table VI. Comparison of cost involved in various combustion technologies [46].

Technology	Cost (Canadian $\$\,MWh^{-1}$)	Plant efficiency (%)	CO_2 emission ($kg\,MWh^{-1}$)	SO_2 emission ($kg\,MWh^{-1}$)	NO_x emission ($kg\,MWh^{-1}$)	Particulate emission ($kg\,MWh^{-1}$)
Subcritical pulverized coal combustion	43.30	33	1000	1.6	2.1	0.5
Supercritical pulverized coal combustion	42.94	38–43	770–870	1.4	1.8	0.4
Atmospheric fluidized bed combustion	42.45	36	920	0.3	0.5	~0.4
Atmospheric fluidized bed combustion with 30% oxygen-containing air	44.91	n/a	n/a	n/a	n/a	n/a
Pressurized fluidized bed combustion	45.58	42	790	0.1	<0.7	0.1–0.5
Integrated gasification combined cycle	46.04	45	735	~0.0	0.3–0.5	~0.0

7. POSSIBLE MODIFICATIONS IN THE DESIGN OF FLUIDIZED BED COMBUSTOR

The FBC technology is a mature technology for industrial applications. Possible areas where future research and development is needed have been indicated by some FBC operators. The three most important areas (in order of importance) for FBC used in industrial applications are materials handling, environmental control technology, and boiler reliability. The operators of FBC technology for utility applications have indicated boiler reliability, fuel flexibility, and environmental control technology as the most important R&D areas [134]. Future development of BFB technology is likely to be limited to ensuring fuel flexibility on existing designs for the increasing use of biomass and/or waste as feedstock with, or instead of, coal. The BFB technology should ensure a firm market share in the niche market of small and cogeneration units. Contrary to CFB, fewer number of major industrially focused international R&D projects are underway for BFB.

There are some inherent problems associated with BFB. Some of these are explained below.

1. The fuel preparation and feeding systems sometimes get jammed and cannot maintain a homogeneous flow [128]. The reason may be that the size of particles is such that the saltation velocity of the large particles is higher than the velocity of gas in some regions of the flow system so that the particles settle down. When the number of such particles becomes large, it may resist flow of solid feeding. Use of large particles reduces the cost of crushing. A compromise of particle size has to be brought because large particles need longer devolatilization time, which may push the combustion of volatiles to the freeboard section of the combustor. It also requires very high transportation velocity and smaller particle size, which will induce more crushing cost. The evolution of volatile matter with time for a batch of feed coal particles can be calculated using the empirical or semi-empirical models. Therefore, the total amount of volatile matter required to be handled can be calculated at any time and the feed size of coal can be determined to obtain the required output.
2. The use of sorbent (lime for combustion of high-sulfur coal) is often higher than that expected [128], which leads to various problems in sorbent feeding and waste disposal. The particle size of the sorbent is higher in the BFB than the CFB. Hence, the surface area of the particles in the BFB is less than the CFB. Hence, the absorption efficiency of sorbent in CFB is higher than BFB. BFB requires more sorbent for similar application. However, smaller particle size requires more crushing power and thereby increases operation cost. The use of oxygen-enriched air can help to convert the calcium sulfite to calcium sulfate. The absorption of sulfur dioxide will also be high. Therefore, by increasing the percentage of oxygen in the fluidizing gas, the absorption efficiency of lime particles can be increased in BFB.
3. Another problem often encountered is that the temperature in the freeboard is higher than that anticipated [128]. As a consequence, the design lacks sufficient heating surface. The reason for this phenomenon is that a major fraction of the volatile matter evolved during devolatilization of coal burns in the freeboard section of the fluidized bed. This increases the temperature of the freeboard more than that anticipated. The volatile matter evolved in fluidized bed is on average 25% higher than the proximate volatile content of coal. The particle size of the coal feed needs to be optimized to reduce burning of volatile matter in the freeboard section of the fluidized bed. Increase in the oxygen content in the fluidizing gas can reduce devolatilization time and increase combustion inside the fluidized bed.
4. The main problem that arises while scaling up BFB is the geometry of the boiler. With increase in the capacity of a BFB boiler, the cross-section of the boiler must be enlarged. This leads to problems in fluidization of the combustion mixture and leads to a shortage of heat transfer surface between the bed and the working fluid [128]. Use of multiple fluidized beds may be a solution to this problem.

Several opportunities remain to support further development of the supercritical CFB and the pressurized CFB [135]. Further developments in improvement of efficiency, fuel flexibility, effective scale-up, and reduction in the capital cost are needed for CFB to remain a competitive technology and gain market share in the utility segment. The total worldwide installed capacity of BFB is surpassed by the capacity of CFB. This is mainly due to the rapid diffusion of CFB, which started in the 1980s. The cost of BFB is lower than CFB and PFBC. With oxygen-enriched air, the cost of BFB is still lower than PFBC [16]. Hence, BFB can be considered as one of the viable options in the power generation applications.

8. CONCLUDING REMARKS

In this review, emphasis has been placed on developing a mechanistic understanding of coal devolatilization and how it relates to the parent coal structure and properties. The structural and mechanistic models not only provide a physicochemical description of the devolatilization process but also form the basis on which observations regarding the influence of various

Int. J. Energy Res. 2011; **35**:929–963 © 2011 John Wiley & Sons, Ltd.
DOI: 10.1002/er

parameters on the devolatilization products can be analyzed and a rationale for the observed effect can be deduced. Devolatilization of large coal particles is complicated and the effect of 10 different parameters has been analyzed. No single parameter can explain the trends observed in the evolution of volatile matter. Temperature is a key parameter for the devolatilization of coal, because the physicochemical transformations of the constituents of coal depend on temperature. The reactions occurring during devolatilization are mostly endothermic. Hence, the heating rate plays an important role in devolatilization. Because the specific heat of coal varies with the volatile content of coal, the coal particles having different specific heat are heated at different rates even though they are exposed to a similar heating condition. As a result, the evolution of volatile matter also differs, and it also depends on the volatile matter content of coal. Coal particles containing the same percentage of volatile matter but of different size are heated at different rates when exposed to similar conditions. When the fluidization velocity is increased, the increase in turbulence accelerates devolatilization and reduces devolatilization time. Increase in pressure in the system increases resistance to diffusion of the volatile products out of the coal particle. Oxygen concentration plays a vital role in the devolatilization of coal. The volatile film at the surface of the coal particle is oxidized in the presence of oxygen releasing sensible heat, which increases heat transfer to the particle, thereby increasing the rate of devolatilization and decreasing the time of devolatilization. Consequently, the devolatilization time decreases as the oxygen concentration increases. Devolatilization is considerably faster in the presence of oxygen-enriched air than inert gas or air. This can increase the combustion efficiency and heat transfer from the bed.

Structural models are effective in predicting the yields of tar and light gas, and production of char during devolatilization. The FG-DVC model can predict cross-linking, hydrogen utilization, and fragmentation during devolatilization. FG-DVC model can be applied to predict the solvent swelling and insolubility behavior of coals. It can distinguish between the evolved tar, solvent extractable, and liquid products generated during devolatilization with reasonable success. The CPD model is generally considered to be more computationally efficient than the FG-DVC model in its treatment of coal structure. However, it is not as sophisticated in its consideration of the structural changes occurring during devolatilization. The quality and quantity of data required for the structural models is high and they are coal-specific as well. This reduces the scope of these models to a unique type of coal that corresponds to the input data. The empirical models are simple in comparison with the structural models. These models assume a simplified overall reaction rate for the entire devolatilization process. Hence, extensive data relating to the structure of the coal are not required. Only kinetic parameters and data on the temperature of the particles are required. The kinetic parameters are sometimes available in literature. In some specific cases, appropriate kinetic data need to be generated. The data required for these models can be obtained with rather simple techniques as compared with that required for the structural models. However, the applicability of the empirical models is limited to devolatilization (i.e. volatile gas and tar evolution) only. These models are not effective in predicting the relative yields of tar, char and volatile gases due to their total independence of the coal structure.

Modeling of devolatilization of large coal particles poses a number of additional challenges to that of the pulverized coal particles. The particle size has a significant effect on the mechanism of coal devolatilization. Large particles effectively increase the residence time of the primary volatiles within the particles, thus providing additional opportunities for subsequent secondary reactions. Modeling of these secondary reactions is complex, and ideally should be coupled with mass transfer equations such that the rate of these reactions and the rate of mass transport of the primary volatiles out of the particle can be considered simultaneously. This substantially increases the complexity of the kinetic model. However, it has been shown that this can be achieved with the use of the FG-DVC model. However, so far the FG-DVC model has not been combined with a sophisticated thermal model for the large particles. It is envisaged that such a model would be highly rigorous but quite complex because of the inclusion of drying, and combustion of volatile matter and char.

In a fluidized bed, the particles are not of the same size and a distribution of particle size exists. Therefore, the operation of fluidized bed requires stochastic modeling. The probabilistic approach allows defining some statistical measures for the variation in size. Therefore, it can be superior to the deterministic empirical models [136]. The statistical modeling of the evolution of volatile matter with respect to particle size and temperature will increase the accuracy of the model. A more complicated issue is the heterogeneous nature of coal, which causes difference in the properties among coals belonging to the same colliery.

The progress ratio for the new FBC plants lies between 0.9 and 0.93. These values correspond with the average progress ratio of 0.9 for power plants reported in the literature. The economy-of-scale has a significant influence on the investment cost. Scale factors are found in the range of 0.62–0.81 for different groups of projects. The specific investment price decreases between 25 and 12% with every doubling of the plant capacity.

The efficiency of BFB can be increased by using oxygen-enriched air. The cost of BFB is lower than

CFB and PFBC. Hence, BFB can still be considered as one of the alternatives in the power generation scenario.

NOMENCLATURE

a = radius of coal particle (m)
A = correlation constant ($s\,mm^{-n}$)
A_1 = correlation constant for air ($s\,mm^{-n_1}$)
A_2 = correlation constant for the parameter C of mass versus time correlation ($s\,mm^{-n_2}$)
A_3 = correlation constant for devolatilization time at different oxygen concentration ($s\,mm^{-n_3}$)
A_d = ash content on dry basis (%)
b = experience index
B_i = Biot number, $B_i = ha/(3k_t)$
c = mean value of concentration of volatile matter assuming a uniform distribution of potential volatile species throughout the particle ($mol\,m^{-3}$)
c_a = constant of proportionality between the rate of transformation of liquid to vapor at the surface of the drop of volatile matter (per unit area) to the rate of shrinkage of the drop of volatile matter ($kg^2\,m^{-2}\,s^{-2}$)
c_{O_2} = concentration of oxygen in the fluidizing gas (%)
C = constant for mass versus time correlation (s^{-M})
C_0 = cost of the first unit ($)
C_{CUM} = cost of a unit after a number of cumulative units are produced ($)
C_{daf} = carbon content on dry ash-free basis (%)
d = diameter of the coal particle (m)
$\hat{d}$ = geometric mean diameter of coal particle (m)
D = effective diffusivity of the volatile matter ($m^2\,s^{-1}$)
E = activation energy ($J\,mol^{-1}$)
h = convective heat transfer coefficient ($W\,m^{-2}\,K^{-1}$)
H_{daf} = hydrogen content on dry ash-free basis (%)
k = rate constant (s^{-1})
k_0 = frequency factor (s^{-1})
k_{di} = decomposition rate of species i (s^{-1})
k_t = thermal conductivity of coal ($W\,m^{-1}\,K^{-1}$)
k_{vi} = rate of evolution of species i (s^{-1})
m = reaction order
M = constant for mass versus time correlation
n = correlation parameter
n_1 = correlation parameter
n_2 = correlation parameter
n_3 = correlation parameter
N_{cum} = cumulative number of units produced
O_{daf} = oxygen content on dry ash-free basis (%)
p = constant ($s^{-1}\,mm^{-q}$)
$\bar{p}$ = ratio of volatile yield to that of proximate volatile content of coal
P = permeability of the char (m^2)
q = constant
r = radial distance from center (m)
r_c = radius of the unreacted core of the coal particle (m)
R = universal gas constant ($J\,mol^{-1}\,K^{-1}$)
$\tilde{R}$ = Pearson correlation coefficient
t = time (s)
t_v = devolatilization time (s)
T = temperature (K)
T_b = temperature of the fluidized bed (K)
v = superficial velocity ($m\,s^{-1}$)
V = volatile matter content at time t ($kg\,kg^{-1}$ of dry coal)
V_0 = mass of coal at $t = 0$ (kg)
V_∞ = mass of coal after devolatilization (i.e. $t = \infty$) (kg)
V_a = mass of coal at time t (kg)
V_{daf} = volatile matter content on dry ash-free basis (%)
V_i = yield of species i ($kg\,kg^{-1}$ of dry coal)
V_m = volatile matter content of coal ($kg\,kg^{-1}$)
V^* = ultimate yield of volatile matter ($kg\,kg^{-1}$ of dry coal)
V_i^* = ultimate yield of species i ($kg\,kg^{-1}$ of dry coal)
x_o = mole fraction of oxygen

Greek symbols

α_c = thermal diffusivity of coal ($m^2\,s^{-1}$)
ΔH = enthalpy of devolatilization ($J\,kg^{-1}$)
ΔT = temperature difference between the fluidized bed and the surface of the unreacted core of radius r_c (K)
ε_r = emissivity
η = viscosity of the flowing volatile matter (Pa s)
ρ = density of virgin coal ($kg\,m^{-3}$)
ρ_v = molar density of volatiles in the particle ($mol\,m^{-3}$)
σ_d = drop density (kgm^{-3})
σ_r = Stefan–Boltzmann's constant ($W\,m^{-2}\,K^{-4}$)

Abbreviations

BFB = bubbling fluidized bed
CFB = circulating fluidized bed
CPD = chemical percolation devolatilization
EPC = engineering, procurement and construction
FBC = fluidized bed combustion

Int. J. Energy Res. 2011; **35**:929–963 © 2011 John Wiley & Sons, Ltd.
DOI: 10.1002/er

FG-DVC = functional group-depolymerization, vaporization and cross-linking model
FIMS = field ionization mass spectrometer
IEA = international energy agency
IGCC = integrated gasification combined cycle
LR = learning ratio
NMR = nuclear magnetic resonance
PCFB = pressurized circulating fluidized bed
PFBC = pressurized fluidized bed combustion
PR = progress ratio
R&D = research and development
TGA = thermogravimetric apparatus
VSR = volumetric swelling ratio

REFERENCES

1. Stach E, Mackowsky M-Th, Teichmüller M, Taylor GH, Chandra D, Teichmüller R. *Stach's Textbook of Coal Petrology*. Gebrüder Borntraeger: Berlin, 1982.
2. Shinn JH. From coal to single-stage and two-stage products: a reactive model of coal structure. *Fuel* 1984; **63**:1187–1196.
3. Solomon PR, Hamblen DG, Serio MA, Yu Z-Z, Charpenay S. A characterization method and model for predicting coal conversion behaviour. *Fuel* 1993; **72**:469–488.
4. Solomon PR, Fletcher TH, Pugmire RJ. Progress in coal pyrolysis. *Fuel* 1993; **72**:587–597.
5. van Heek KH, Hodek W. Structure and pyrolysis behaviour of different coals and relevant model substances. *Fuel* 1994; **73**:886–896.
6. Jüntgen H. Review of the kinetics of pyrolysis and hydropyrolysis in relation to the chemical constitution of coal. *Fuel* 1984; **63**:731–737.
7. Serio MA, Hamblen DG, Markham JR, Solomon PR. Kinetics of volatile product evolution in coal pyrolysis: experiment and theory. *Energy and Fuels* 1987; **1**:138–152.
8. Hayashi J, Nakagawa K, Kusakabe K, Morooka S. Change in molecular structure of flash pyrolysis tar by secondary reaction in a fluidized bed reactor. *Fuel Processing Technology* 1992; **30**:237–248.
9. Pather TS, Al-Masry WA. The influence of bed depth on secondary reactions during slow pyrolysis of coal. *Journal of Analytical and Applied Pyrolysis* 1996; **37**:83–94.
10. Hesp R, Waters PL. Thermal cracking of tars and volatile matter from coal carbonization. *Industrial and Engineering Chemistry Product Research and Development* 1970; **9**:194–202.
11. Niksa S. Modeling the devolatilization behavior of high volatile bituminous coals. *Proceedings of the Combustion Institute*. Washington, 1989; 105–114.
12. Xu W-C, Tomita A. The effects of temperature and residence time on the secondary reactions of volatiles from coal pyrolysis. *Fuel Processing Technology* 1989; **21**:25–37.
13. Stiles HN, Kandiyoti R. Secondary reactions of flash pyrolysis tars measured in a fluidized bed pyrolysis reactor with some novel design features. *Fuel* 1989; **68**:275–282.
14. Jess A. Mechanisms and kinetics of thermal reactions of aromatic hydrocarbons from pyrolysis of solid fuels. *Fuel* 1996; **75**:1441–1448.
15. Stubington JF, Sumaryono A. Release of volatiles from large coal particles in a hot fluidized bed. *Fuel* 1984; **63**:1013–1019.
16. Borah RC, Rao PG, Ghosh P. Devolatilization of coals of northeastern India in inert atmosphere and in air under fluidized bed conditions. *Fuel Processing Technology* 2010; **91**:9–16.
17. Stubington JF, Ng KWK, Moss B, Peeler PK. Comparison of experimental methods for determining coal particle devolatilization times under fluidized bed combustor conditions. *Fuel* 1997; **76**:233–240.
18. Xu W-C, Tomita A. Effect of temperature on the flash pyrolysis of various coals. *Fuel* 1987; **66**:632–636.
19. Tyler RJ. Flash pyrolysis of coals: 1. Devolatilization of a Victorian brown coal in a small fluidized-bed reactor. *Fuel* 1979; **58**:680–686.
20. Suuberg EM, Peters WA, Howard JB. Product compositions and formation kinetics in rapid pyrolysis of pulverized coal—implications for combustion. *Proceedings of the Combustion Institute*, Leeds, 1979; 117–130.
21. Tyler RJ. Flash pyrolysis of coals: devolatilization of bituminous coals in a small fluidized-bed reactor. *Fuel* 1980; **59**:218–226.
22. Cliff DI, Doolan KR, Mackie JC, Tyler RJ. Products from rapid heating of a brown coal in the temperature range 400–2300°C. *Fuel* 1984; **63**:394–400.
23. Xiong R, Dong L, Yu J, Zhang X, Jin L, Xu G. Fundamentals of coal topping gasification: characterization of pyrolysis topping in a fluidized bed reactor. *Fuel Processing Technology* 2010; **91**:810–817.
24. Calkins WH, Hagaman H, Zeldes H. Coal flash pyrolysis: 1. An indication of the olefin precursors in coal by CP/MAS ^{13}C n.m.r. spectroscopy. *Fuel* 1984; **63**:1113–1118.

25. Ladner WR. The products of coal pyrolysis: properties, conversion and reactivity. *Fuel Processing Technology* 1988; **20**:207–222.
26. Gokhale AJ, Vasudevan TV, Mahalingam R. Parametric studies on devolatilization of a subbituminous coal in a reactive gas environment. *Fuel* 1986; **65**:1670–1676.
27. Shin Y, Choi S, Ahn D-H. Pressurized drop tube furnace tests of global coal gasification characteristics. *International Journal of Energy Research* 2000; **24**:749–758.
28. Cho HC, Cho KW, Lee YK, Shin HD, Ahn DH. Effect of coal type on gasification in pressurized drop tube furnace. *International Journal of Energy Research* 2001; **25**:427–438.
29. Niksa S, Heyd LE, Russel WB, Saville DA. On the role of heating rate in rapid coal devolatilization. *Proceedings of the Combustion Institute*, Michigan, 1985; 1445–1453.
30. Peters W, Bertling H. Kinetics of the rapid degasification of coals. *Fuel* 1965; **44**:317–331.
31. Akash BA, O'Brien WS. The production of activated carbon from a bituminous coal. *International Journal of Energy Research* 1996; **20**: 913–922.
32. Loison R, Chauvin R. Rapid pyrolysis of coal. *Chimie et Industrie* 1964; **91**:269–275.
33. Jones JF, Schmid MR, Eddinger RT. Fluidized-bed pyrolysis of coal. *Chemical Engineering Progress* 1964; **60**:69–73.
34. Eddinger RT, Friedman LT, Rau E. Devolatilization of coal in a transport reactor. *Fuel* 1966; **45**:245–252.
35. Rau E, Robertson JA. The use of the micro-sample strip furnace in coal research. *Fuel* 1966; **45**:73–80.
36. Mentser M, O'Donnell HJ, Ergun S. Rapid thermal decomposition of bituminous coals. *American Chemical Society*, *Division of Fuel Chemistry* 1970; **14**:94–100.
37. Anthony DB, Howard JB, Hottel HC, Meissner HP. Rapid devolatilization of pulverized coal. *Proceedings of the Combustion Institute*, Tokyo, 1975; 1303–1317.
38. Gavalas GR. Coal pyrolysis. In *Coal Science and Technology*, Anderson LL (ed.), vol. 4. Elsevier: New York, 1982; 66–69.
39. Stubington JF, Sasongko D. On the heating rate and volatile yield for coal particles injected into fluidised bed combustors. *Fuel* 1998; **77**: 1021–1025.
40. Arendt P, van Heek K-H. Comparative investigations of coal pyrolysis under inert gas and H_2 at low and high heating rates and pressures up to 10 MPa. *Fuel* 1981; **60**:779–787.
41. Ross DP, Heidenreich CA, Zhang DK. Devolatilization times of coal particles in a fluidised-bed. *Fuel* 2000; **79**:873–883.
42. Smoot LD, Smith PJ. *Coal Combustion and Gasification*. Plenum Press: New York, 1985.
43. Morris RM. Effect of particle size and temperature on evolution rate of volatiles from coal. *Journal of Analytical and Applied Pyrolysis* 1993; **2**:97–107.
44. Morris RM. Effect of particle size and temperature on volatiles produced from coal by slow pyrolysis. *Fuel* 1990; **69**:776–779.
45. Griffin TP, Howard JB, Peters WA. An experimental and modeling study of heating rate and particle size effects in bituminous coal pyrolysis. *Energy and Fuels* 1993; **7**:297–305.
46. Borah RC, Ghosh P, Rao PG. Devolatilization of coals of north-eastern India under fluidized bed conditions in oxygen-enriched air. *Fuel Processing Technology* 2008; **89**:1470–1478.
47. Tia S, Bhattacharya SC, Wibulswas P. Spouted and spout-fluid bed combustors 1: devolatilization and combustion of coal volatiles. *International Journal of Energy Research* 1991; **15**:185–201.
48. Morris JP, Keairns DL. Coal devolatilization studies in support of the Westinghouse fluidized-bed coal gasification process. *Fuel* 1979; **58**: 465–471.
49. Stubington JF, Chui TY, Saisthidej S. Experimental factors affecting devolatilization time in fluidized bed combustion. *Fuel Science and Technology International* 1992; **10**:397–419.
50. Zhang JQ, Becker HA, Code RK. Devolatilization and combustion of large coal particles in a fluidized bed. *Canadian Journal of Chemical Engineering* 1990; **68**:1010–1017.
51. Winter F, Prah ME, Hofbauer H. Temperature in a fuel particle burning in a fluidized bed: the effect of drying, devolatilization and char combustion. *Combustion and Flame* 1997; **108**: 302–314.
52. Oka SN. *Fluidized Bed Combustion*. Dekker: New York, 2004.
53. Chen W-H, Chen J-C, Tsai C-D, Jiang TL. Transient gasification and syngas formation from coal particles in a fixed-bed reactor. *International Journal of Energy Research* 2007; **31**:895–211.
54. Zhenfu L, Qingru C. Dry beneficiation technology of coal with an air dense-medium fluidized bed. *International Journal of Mineral Processing* 2001; **63**:167–175.

55. Stubington JF, Huang G, Scaroni AW. Devolatilization times of mm-size coal particles. *Fuel* 1991; **70**:105–1108.
56. Jia L, Becker HA, Code RK. Devolatilization and char burning of coal particles in a fluidized bed combustor. *Canadian Journal of Chemical Engineering* 1993; **71**:11–19.
57. Salam TF, Shen XL, Gibbs BM. A technique for determining devolatilization rates of large coal particles in a fluidized bed combustor. *Fuel* 1988; **67**:414–419.
58. Tomeczek J, Palugniok H. Specific heat capacity and enthalpy of coal pyrolysis at elevated temperatures. *Fuel* 1996; **75**:1089–1093.
59. Zhang H, Cen K, Yan J, Ni M. The fragmentation of coal particles during the coal combustion in a fluidized bed. *Fuel* 2002; **81**:1835–1840.
60. LaNauze RD. Coal devolatilization in fluidized bed combustors. *Fuel* 1982; **61**:771–774.
61. Stubington JF. The role of coal volatiles in fluidized bed combustion. *Journal of the Institute of Energy* 1980; **53**:191–195.
62. Bywater RJ. The effects of devolatilization kinetics on the injector region of fluidized beds. *Proceedings of the Sixth International Conference on Fluidized Bed Combustion*, Atlanta, 1980; 1092–1102.
63. Leckner B, Lyngfelt A. Optimization of emissions from fluidized bed combustion of coal, biofuel and waste. *International Journal of Energy Research* 2002; **26**:1191–1202.
64. Feng B, Liu H, Yuan J-W, Lin Z-J, Liu D-C, Leckner B. Nitrogen oxides emission from a circulating fluidized bed combustor. *International Journal of Energy Research* 1996; **20**:1015–1025.
65. Stubington JF, Linjewile TM. The effects of fragmentation on devolatilization of large coal particles. *Fuel* 1989; **68**:155–160.
66. Agarwal PK, LaNauze RD. Transfer processes local to the coal particle: a review of drying, devolatilization and mass transfer in fluidized bed combustion. *Chemical Engineering Research and Design* 1989; **67**:457–480.
67. Borghi G, Sarofim A, Beer JM. A model of coal devolatilization and combustion in fluidized beds. *Combustion and Flame* 1985; **61**:1–16.
68. Borah RC, Mazumder B, Bora MM. Atmospheric fluidized bed combustion of high sulphur high volatile N.E. Region coals of India. *Research and Industry* 1995; **40**:315–321.
69. Atimtay AT, Varol M. Investigation of co-combustion of coal and olive cake in a bubbling fluidized bed with secondary air injection. *Fuel* 2009; **88**:1000–1008.
70. Agarwal PK, Wildegger-Gaissmaier AE. Combustion of coal volatiles in gas fluidized beds. *Chemical Engineering Research and Design* 1987; **65**:431–441.
71. Stubington JF, Chan SW. On the phase location and rate of volatiles combustion in bubbling fluidized bed combustors. *Chemical Engineering Research and Design* 1990; **68**:195–201.
72. Johnsson JE. Formation and reduction of nitrogen oxides in fluidized-bed combustion. *Fuel* 1994; **73**:1398–1415.
73. García-Labiano F, Adánez J, Hampartsoumian E, Williams A. Sulfur release during the devolatilization of large coal particles. *Fuel* 1996; **75**: 585–590.
74. Memon HUR, Williams A, Williams PT. Shock tube pyrolysis of thiophene. *International Journal of Energy Research* 2003; **27**:225–239.
75. Peeler JPK, Poynton HJ. Devolatilization of large coal particles under fluidized bed conditions. *Fuel* 1992; **71**:425–430.
76. Zhang JQ, Becker HA, Code RK. Experimental study on devolatilization of large coal particles in a fluidized bed. *Proceedings of the Ninth International Conference on Fluidized Bed Combustion*, Boston, 1987; 1203–1210.
77. Saito M, Sadakata M, Saka T. Measurements of surface combustion rate of single coal particles in laminar flow furnace. *Combustion Science and Technology* 1987; **51**:109–128.
78. Essenhigh RH. Influence of coal rank on the burning times of single captive particles. *Journal of Engineering for Power* 1963; **85**:183–190.
79. Jung K, Stanmore BR. Fluidized bed combustion of wet brown coal. *Fuel* 1980; **59**:74–80.
80. Pillai KK. Influence of coal type on devolatilization and combustion in fluidized beds. *Journal of the Institute of Energy* 1981; **54**:142–150.
81. Ragland KW, Weiss CA. Combustion of single coal particle in a jet. *Energy* 1979; **4**:341–348.
82. Grant DM, Pugmire RJ, Fletcher TH, Kerstein AR. Chemical model of coal devolatilization using percolation lattice statistics. *Energy and Fuels* 1989; **3**:175–186.
83. Solomon PR, Hamblen DG, Carangelo RM, Serio MA, Deshpande GV. A general model of coal devolatilization. *Energy and Fuels* 1988; **2**:405–422.
84. Niksa S, Kerstein AR. Flashchain theory for coal devolatilization kinetics: 1. Formulation. *Energy and Fuels* 1991; **5**:647–665.
85. Fletcher TH, Kerstein AR, Pugmire RJ, Solum MS, Grant DM. A chemical percolation model for

devolatilization: 3. Chemical structure as a function of coal type. *Energy and Fuels* 1992; **6**:414–431.
86. Jupudi RS, Zamansky V, Fletcher TH. Prediction of light gas composition on coal devolatilization. *Energy and Fuels* 2009; **23**:3063–3067.
87. Serio MA, Hamblen DG, Markham JR, Solomon PR. Kinetics of volatile product evolution in coal pyrolysis: experiment and theory. *Energy and Fuels* 1987; **1**:138–152.
88. Solomon PR, Hamblen DG, Yu ZZ, Serio MA. Network models of coal thermal decomposition. *Fuel* 1990; **69**:754–763.
89. Suuberg EM, Lee D, Larsen JW. Temperature dependence of cross-linking processes in pyrolysis of coal. *Fuel* 1985; **64**:1668–1671.
90. Fong WS, Peters WA, Howard JB. Kinetics of generation and destruction of pyridine extractable in a rapidly pyrolysing bituminous coal. *Fuel* 1986; **65**:251–254.
91. Solomon PR, Hamblen DG, Deshpande GV, Serio MA. Modeling chemical and physical processes of wood and biomass pyrolysis. In *Coal Science and Technology*, Moulijn JA, Nater KA, Chermin HAG (eds), vol. 11. Elsevier: Amsterdam, 1987; 601–611.
92. Serio MA, Solomon PR, Yu ZZ, Deshpande GV, Hamblen DG. Pyrolysis modeling of the argonne premium coals. *American Chemical Society, Fuel Chemistry Division* 1988; **33**:91–101.
93. Serio MA, Solomon PR, Yu ZZ, Deshpande GV, Hamblen DG. An improved model of coal devolatilization. *Proceedings of the International Conference on Coal Science*, Tokyo, 1989; 209–217.
94. Carangelo RM, Solomon PR, Gerson DJ. Application of TG-FTIR to study hydrocarbon structure and kinetics. *Fuel* 1987; **66**:960–967.
95. Nelson JR. Determination of molecular weight between cross links of coals from solvent-swelling studies. *Fuel* 1983; **62**:112–116.
96. Solomon PR, Squire KR. Experiments and modeling of coal depolymerization. *American Chemical Society*, *Fuel Chemistry Division* 1985; **30**:346–356.
97. St. John GA, Butrill Jr SE, Anbar M. Field ionization and field desorption mass spectrometry applied to coal research. In *Organic Chemistry of Coal* (*ACS Symposium Series*), Larsen JW (ed.), vol. 71. American Chemical Society: Washington, 1978; 223–239.
98. Zhao Y, Serio MA, Bassilakis R, Solomon PR. A method of predicting coal devolatilization behavior based on the elemental composition. *Proceedings of the Combustion Institute*, California, 1994; 553–560.
99. van Krevelen DW, Huntjens FJ, Dormans HNM. Chemical structure and properties of coal: XVI. Plastic behavior on heating. *Fuel* 1956; **35**: 462–475.
100. Stone HN, Batchelor JD, Johnstone HF. Low-temperature carbonization rates in a fluidized bed. *Journal of Industrial and Engineering Chemistry* 1954; **46**:274–278.
101. Howard JB, Essenhigh RH. Pyrolysis of coal particles in pulverized fuel flames. *Industrial and Engineering Chemistry Process Design and Development* 1967; **6**:74–84.
102. Wiser WH, Hill GR, Kertamus NJ. Kinetic study of the pyrolysis of a high-volatile bituminous coal. *Industrial and Engineering Chemistry Process Design and Development* 1967; **6**:133–138.
103. Badzioch S, Hawksley PGW. Kinetics of thermal decomposition of pulverized coal particles. *Industrial and Engineering Chemistry Process Design and Development* 1970; **9**:521–530.
104. Kobayashi H, Howard JB, Sarofim AF. Coal devolatilization at high temperatures. *Proceedings of the Combustion Institute*, Massachusetts, 1977; 411–425.
105. Maloney DJ, Jenkins RG. Coupled heat and mass transport and chemical kinetic rate limitations during coal rapid pyrolysis. *Proceedings of the Combustion Institute*, Michigan, 1985; 1435–1443.
106. Sandhu SS, Hashemi HR. A model for simultaneous heating and devolatilization of a single coal particle in a hot gas stream in the presence of a thermal radiative field. *American Institute of Chemical Engineers Journal* 1985; **31**:1714–1717.
107. Fu W, Zhang Y, Han H, Duan Y. A study on devolatilization of large coal particles. *Combustion and Flame* 1987; **70**:253–266.
108. Sharma DK, Sarkar MK, Ganapathi M. Kinetics studies of the devolatilization of Indian coals in isothermal and nonisothermal conditions in thermobalance and in a batch reactor. *Fuel Science and Technology International* 1994; **12**:795–811.
109. Li Y, Lu GQ, Rudolph V. A kinetic study on pyrolysis of Australian coals by thermogravimetric analysis. *Proceedings of the 24th Australian and New Zealand Chemical Engineering Conference and Exhibition* (*Chemeca 96*), Sydney, 1996; 143–148.
110. Doolan KR, Mackie JC, Mulcahy MFR, Tyler RJ. Kinetics of rapid pyrolysis and hydropyrolysis of a sub-bituminous coal. *Proceedings of the Combustion Institute*, Haifa, 1982; 1131–1138.
111. Yang JT, Wang GG. The effect of heat transfer on coal devolatilization. *Journal of Heat Transfer* 1990; **12**:192–200.

112. Jamaluddin AS, Truelove JS, Wall TF. Modeling of coal devolatilization and its effect on combustion calculations. *Combustion and Flame* 1985; **62**:85–89.
113. Tomeczek J, Kowol J. Temperature field within a devolatilizing coal particle. *Canadian Journal of Chemical Engineering* 1991; **69**:286–293.
114. Agarwal PK, Genetti WE, Lee YY. Model for devolatilization of coal particles in fluidized beds. *Fuel* 1984; **63**:1157–1165.
115. Agarwal PK, Genetti WE, Lee YY. Devolatilization of large coal particles in fluidized beds. *Fuel* 1984; **63**:1748–1752.
116. Agarwal PK. Distributed kinetic parameters for methane evolution during coal pyrolysis. *Fuel* 1985; **64**:870–872.
117. Agarwal PK. A single particle model for the evolution and combustion of coal volatiles. *Fuel* 1986; **65**:803–810.
118. Agarwal PK, Agnew JB, Ravindran N, Weimann R. Distributed kinetic parameters for the evolution of gaseous species in the pyrolysis of coal. *Fuel* 1987; **66**:1097–1106.
119. Wildegger-Gaissmaier AE, Agarwal PK. Drying and devolatilization of large coal particles under combustion conditions. *Fuel* 1990; **69**:44–52.
120. Jie W, Cao Y, Yan Y, Gao J. Heat transfer and kinetics of lignite devolatilization in wire-mesh apparatus. *Fuel Processing Technology* 1994; **38**:57–67.
121. Adesanya BA, Pham HN. Mathematical modeling of devolatilization of large coal particles in a convective environment. *Fuel* 1995; **74**:896–902.
122. Miura K. A new and simple method to estimate $f(E)$ and $k_0(E)$ in the distributed activation energy model from three sets of experimental data. *Energy and Fuels* 1995; **9**:302–307.
123. Maki T, Takatsuno A, Miura K. Analysis of pyrolysis reactions of various coals including Argonne Premium coals using a new distributed activation energy model. *Energy and Fuels* 1997; **11**:972–977.
124. Chern JS, Hayhurst AN. Does a large coal particle in a hot fluidised bed lose its volatile content according to the shrinking core model? *Combustion and Flame* 2004; **139**:208–221.
125. Tia S, Bhattacharya SC, Wibulswas P. Pyrolysis and volatile combustion of a single large lignite particle. *Energy* 1991; **16**:1131–1146.
126. Zedtwitz PV, Lipiński W, Steinfeld A. Numerical and experimental study of gas–particle radiative heat exchange in a fluidized-bed reactor for steam-gasification of coal. *Chemical Engineering Science* 2007; **62**:599–607.
127. Jüntgen H, van Heek KH. An update of German non-isothermal coal pyrolysis work. *Fuel Processing Technology* 1979; **2**:261–293.
128. Koornneef J, Junginger M, Faaij A. Development of fluidized bed combustion—an overview of trends, performance and cost. *Progress in Energy and Combustion Science* 2007; **33**:19–55.
129. International Energy Agency. *Experience Curves for Energy Technology Policy*. OECD: Paris, France, 2000.
130. Lundvall BA. *National Systems of Innovation—Towards a Theory of Innovation and Interactive Learning*. Pinter: London, 1992.
131. Neij L. Dynamics of energy systems—methods of analyzing technology change. *Ph.D. Thesis*. Department of Environmental and Energy System Studies, Lund University, 1999.
132. Alstom Power Inc. *Greenhouse Gas Emissions Control by Oxygen Firing in Circulating Fluidized Bed Boilers. PPL Report No. PPL-03-CT-09*. US Department of Energy: Pennsylvania, PA, 2003; 340–375.
133. Wong R, Whittingham E. *A Comparison of Combustion Technologies for Electricity Generation*. The Pembina Institute: Canada, 2006; 23–37.
134. Fuller JA. Combustion technology research and development issues. *The US Department of Energy Combustion Technology University Alliance Workshop*, Department of Management, West Virginia University, 2003.
135. Hupa M, Zevenhoven M (eds). *Fluidised Bed Conversion—Year Report 2003*, IEA, 2004.
136. Badescu V, Andresen B. Probabilistic finite time thermodynamics: a chemically driven engine. *Journal of Non-Equilibrium Thermodynamics* 1996; **21**:291–306.